ESC European Society of Cardiology

Cardiovascular Research (2018) **114**, 805–821
doi:10.1093/cvr/cvy033

Cardiomyocyte-specific deletion of *Sirt1* gene sensitizes myocardium to ischaemia and reperfusion injury

Lin Wang[1,2], Nanhu Quan[1,2], Wanqing Sun[2], Xu Chen[2], Courtney Cates[2], Thomas Rousselle[2], Xinchun Zhou[3], Xuezhong Zhao[1]*, and Ji Li[2]*

[1]Department of Cardiovascular Center, The First Hospital of Jilin University, Xinmin Street, Changchun 130021, China; [2]Department of Physiology and Biophysics, Mississippi Center for Heart Research, University of Mississippi Medical Center, 2500 N State Street, Jackson, MS 39216, USA; and [3]Department of Pathology, Cancer Institute, University of Mississippi Medical Center, Jackson, MS 39216, USA

Received 9 August 2017; revised 25 December 2017; editorial decision 24 January 2018; accepted 1 February 2018; online publish-ahead-of-print 2 February 2018

Time for primary review: 42 days

Aims A longevity gene, Sirtuin 1 (SIRT1) and energy sensor AMP-activated protein kinase (AMPK) have common activators such as caloric restriction, oxidative stress, and exercise. The objective of this study is to characterize the role of cardiomyocyte SIRT1 in age-related impaired ischemic AMPK activation and increased susceptibility to ischemic insults.

Methods and results Mice were subjected to ligation of left anterior descending coronary artery for *in vivo* ischemic models. The glucose and fatty acid oxidation were measured in a working heart perfusion system. The cardiac functions by echocardiography show no difference in young wild-type C57BL/6J (WT, 4–6 months), aged WT C57BL/6J (24–26 months), and young inducible cardiomyocyte-specific SIRT1 knockout (icSIRT1 KO) (4–6 months) mice under physiological conditions. However, after 45 mins ischaemia and 24-h reperfusion, the ejection fraction of aged WT and icSIRT1 KO mice was impaired. The aged WT and icSIRT1 KO hearts vs. young WT hearts also show an impaired post-ischemic contractile function in a Langendorff perfusion system. The infarct size of aged WT and icSIRT1 KO hearts was larger than that of young WT hearts. The immunoblotting data demonstrated that aged WT and icSIRT1 KO hearts vs. young WT hearts had impaired phosphorylation of AMPK and downstream acetyl-CoA carboxylase during ischaemia. Intriguingly, AMPK upstream LKB1 is hyper-acetylated in both aged WT and icSIRT1 KO hearts; this could blunt activation of LKB1, leading to an impaired AMPK activation. The working heart perfusion results demonstrated that SIRT1 deficiency significantly impaired substrate metabolism in the hearts; fatty acid oxidation is augmented and glucose oxidation is blunted during ischaemia and reperfusion. Adeno-associated virus (AAV9)-Sirt1 was delivered into the aged hearts *via* a coronary delivery approach, which significantly rescued the protein level of SIRT1 and the ischemic tolerance of aged hearts. Furthermore, AMPK agonist can rescue the tolerance of aged heart and icSIRT1 KO heart to ischemic insults.

Conclusions Cardiac SIRT1 mediates AMPK activation *via* LKB1 deacetylation, and AMPK modulates SIRT1 activity *via* regulation of NAD^+ level during ischaemia. SIRT1 and AMPK agonists have therapeutic potential for treatment of aging-related ischemic heart disease.

Keywords Myocardial infarction • SIRT1 • AMP-activated protein kinase • Metabolism

1. Introduction

The *Sirt1* gene belongs to the family of nicotinamide adenine dinucleotide (NAD^+)-dependent proteins and is considered a major gatekeeper against oxidative stress and cardiovascular aging.[1–3] SIRT1 protects the heart from ischaemia/reperfusion injury and cardiomyocyte apoptosis.[2,4] Recently, the longevity protein SIRT1 was proposed to be involved in the metabolic regulation of AMP-activated protein kinase (AMPK) in

* Corresponding authors. Tel: +11 86 431 8878 2222, E-mail: zhxzhzxz@163.com (X.Z.); Tel: +601 815 3987, Fax: 601-984-1817, E-mail: jli3@umc.edu (J.L.)

skeletal muscle, liver, adipose tissue, and pancreatic β cells.[5,6] Moreover, the aging process itself has been described as being associated with a decline in the activity of both SIRT1 and AMPK.[2,7]

AMPK is a conserved energy sensor that regulates cellular metabolism. In general, activation of AMPK results in the repression of ATP-consuming anabolic processes and activation of ATP-producing catabolic processes to maintain cellular energy storage. AMPK can phosphorylate transcription factors and co-activators that regulate gene expression, including FoxO3, PGC1-α, p300, and HNF4. Interestingly, many of these transcription factors are also regulated by SIRT1. Moreover, genetic mutations in AMPK genes cause metabolic disorders in both cardiac[8] and skeletal muscle,[9] suggesting that alterations in AMPK have clinical consequences and may contribute to the decline in stress tolerance observed with aging. SIRT1 has been implicated with the pivotal 'energy switch' protein AMPK; there are studies indicating that SIRT1 may induce AMPK phosphorylation by activating one of its upstream activators LKB1.[10,11] Alternatively, other studies demonstrate that AMPK can activate SIRT1 by elevating intracellular NAD^+ levels.[6,12] Moreover, the effects of both AMPK and SIRT1 on peroxisome proliferator-activated receptor γ coactivator 1-α (PGC1-α) suggest that an interdependence of these two proteins contribute to the stress response and metabolism.[13] Although it has recently become appreciated that both AMPK and SIRT1 are evolutionarily conserved metabolic stress sensors whose functions are complementary,[6] there are findings[14,15] that suggest these two signalling pathways are even more inextricably linked than previously appreciated. This prompts the need for addressing the role of both AMPK and SIRT1 in energy stress of the heart.

We have also reported that aging causes impaired cardiac AMPK signalling in response to ischemic stress.[16] There is mounting evidence that AMPK plays a role in modulating the metabolism of both glucose and fatty acids that may benefit the tolerance of the heart to ischemic stress.[17–19] Therefore, we attempt to elucidate the role of impaired ischaemia and reperfusion (I/R)-induced activation of both AMPK and SIRT1 in the aged heart. Furthermore, we explore whether the small molecule AMPK agonist or SIRT1 agonist can improve cardiac performance in older individuals and augment the aged heart's resistance to ischemic stress by enhancing the cardiac AMPK-SIRT1 signalling cascade.

2. Methods

2.1 Experimental animals

AMPK kinase dead (AMPK KD, α2 K45R mutation, driven in heart and skeletal muscles by the muscle creatine kinase promoter) mice were gifted from Dr Morris Birnbaum.[20] All animal protocols in this study were approved by the University of Mississippi Medical Center Institutional Animal Care and Use Committee. Aged wild-type (WT) (C57BL/6 J, 24–26 months) were purchased from Charles River. Young WT (C57BL/6 J, 4–6 months), $SIRT1^{flox/flox}$ mice (stock number 008041), and $CreER^{T2}$ (stock number 005657) mice were from Jackson Laboratory. Cardiomyocyte-specific deletion of the *SIRT1* gene mouse was generated by breeding $SIRT1^{flox/flox}$ mice with transgenic mice that carried an autosomally integrated *Cre* gene driven by the cardiac-specific alpha-myosin heavy chain promoter (αMHC) ($CreER^{T2}$). The genotyping of mice was performed in the following way: genomic DNA was isolated with the Mouse Tail Quick Extraction kit (BioPioneer) from tail. The inducible cardiac-specific SIRT1 knockout (icSIRT1 KO) mice were generated by Tamoxifen injection (0.08 mg/g, i.p. 5 days) of $CreER^{T2}$-$SIRT1^{flox/flox}$ (12 week old) mice, and $CreER^{T2}$ mice (12 week old) with Tamoxifen injection were used for control groups. The genotying details were descibed in the Supplementary material online. All mice used for the experimental tests were males. All animal experiments were performed in compliance with NIH guidelines.

2.2 *In vivo* regional ischaemia and myocardial infarct size measurements

Mice were anesthetized with isoflurane (2%) *via* inhalation and kept ventilated (Harvard Rodent Ventilator; Harvard Apparatus, Holliston, MA) during surgeries. The body temperature was maintained at 37°C with a heating pad. After left lateral thoracotomy, the left anterior descending coronary artery (LAD) was occluded for ischaemia with an 8-0 nylon suture and polyethylene tubing to prevent arterial injury. An ECG and blanching of the left ventricle confirmed ischemic repolarization changes (ST-segment elevation) during coronary occlusion. At the endpoints of experiments, mice were anesthetized with isoflurane (2%) and ventilated while the hearts were excised, and the ischemic region of the left ventricle was separated before freeze clamping in liquid nitrogen. Freeze-clamped heart tissues were stored at -80°C until further immunoblotting analysis. The myocardial infarct size was calculated as the area of myocardial necrosis as a percentage of the whole area of myocardium. After left lateral thoracotomy, the left anterior descending coronary artery was occluded for 45 min with an 8-0 nylon suture and polyethylene tubing to prevent arterial injury and then reperfused for 24 h. An ECG and blanching of the left ventricle confirmed ischemic repolarization changes (ST-segment elevation) during coronary occlusion (ADInstruments Inc, Colorado Springs, CO). The hearts were then excised, and stained with 2,3,5-triphenyltetrazolium (TTC) and Evans blue dye to delineate the extent of myocardial necrosis as a per cent of the ischemic area at risk (AAR). Hearts were then fixed, sectioned, photographed with a Leica microscope, and analysed with the National Institute of Health's Image J Software.[21,22]

2.3 Microarray analysis

Total RNA was extracted using the Invisorb RNA Kit II (Invitek, Berlin, Germany) according to the manufacturer's instructions, and microarray was performed with use of the Genomic Shared Resource in Roswell Park Cancer Institute. The Illumina MouseWG-6 v2.0 R2 expression beadchip (gene symbol version, GPL22165) was used for determining $SIRT1^{flox/flox}$ or icSIRT1 KO samples. Gene sets were imported into the Protein Analysis through Evolutionary Relationship (PANTHER v10.0) Classification System and searched to detect statistically over-represented pathways. Microarray data were deposited in the Gene Expression Omnibus (GEO) database (accession No. GSE98749) while following the Minimum Information regarding Microarray Experiments (MIAME).

2.4 *In vivo* evaluation of heart function by echocardiography

Four weeks after surgery, representative randomly selected animals from each group were anaesthetized (isoflurane) and transthoracic M-mode echocardiography (Vevo770, Visualsonics, Toronto) was performed to measure cardiac function, wall thickness, and chamber volumes. Left ventricle (LV) wall thickness was measured using a modified version of the leading-edge method of the American Society for Echocardiography using three consecutive cycles of M-mode tracing. Myocardial peak velocities (systolic and diastolic) were measured at the mitral valve level, and the ratio between early mitral inflow velocity and

mitral annular early diastolic velocity (*E*/*E*′) ratio was used as an indicator of LV filling pressure.[23] Other indicators of diastolic function that were also calculated include isovolumetric relaxation time (IVRT), mitral valve deceleration time (MVDT), ratio of early (*E*), and late (*A*) mitral inflow velocities (*E*/*A*), and Tei index [calculated as sum of isovolumetric relation and contraction times (IVRT + IVCT) divided by ejection time (ET)]. Simpson's measurements were performed to obtain an average ejection fraction (%EF) and fractional shortening (%FS) of all coronary artery ligation animals and 6 representative samples of the Sham group. Only a representative sample of Sham hearts was required since wall motions were observed to have synchronous motion, whereas infarcted group had asynchronous wall motion. Since all coronary artery ligation mice were expected to have infarcts and asynchronous wall motion, the averaged %EF and %FS were calculated using Simpson's measurements.

2.5 Adeno-associated viral delivery

Mice were anesthetized with isoflurane (2%) and placed on a ventilator. The chest was entered from the left side through the forth intercostal space. The pericardium was opened and 7-0 suture placed at the apex of the left ventricle. After dissection of the aorta and pulmonary artery, the adeno-associated virus (AAV9, 5×10^7 gc per mouse) was injected into the left ventricular cavity through a 27-G catheter while the aorta and pulmonary artery were crossed-clamped for 50 s. In sham-operated animals, normal saline was injected into the left ventricular cavity while the aorta and pulmonary artery were crossed-clamped for 50 s. This procedure allows the solution that contains the adeno-associated virus (AAV9) to circulate down the coronary arteries and perfuse the heart without direct manipulation of the coronaries. After 50 s, the clamp on the aorta and pulmonary artery was released. After removal of air and blood, the chest was closed, and animals were extubated and transferred back to the cages.

2.6 Immunoblotting

Immunoblots and immunoprecipitation were performed as previously described.[24–26] Rabbit antibodies p-AMPKα (Thr^{172}), AMPKα, p-acetyl-CoA carboxylase (ACC) (Ser^{79}), ACC, Eukaryotic elongation factor 2 (p-eEF2), phosphor-Serine/threonine-protein kinase ULK1 (Ser^{555}), glyceraldehyde 3-phosphate dehydrogenase (GAPDH), PGC-1α, TUG, and LKB1 were obtained from Cell Signaling Tech (Danvers, MA). Goat LKB1 (M-18) was obtained from Santa Cruz Technology (Santa Cruz, CA). Mouse LKB1 antibody was obtained from Novus Biologicals (Littleton, CO). 4-Hydroxynonenal (4-HNE) antibody was purchased from Abcam (Cambridge, MA). The quantification of phosphor/total signalling proteins was normalized to an internal loading control before calculating the ratio of phosphor/total proteins.

2.7 Relative quantification of mtDNA copy number

Total DNA was isolated from hearts of young WT, aged WT, and icSIRT1 KO mice and treated with RNase A (Invitrogen). The mtDNA content relative to nuclear DNA was assessed by real-time qPCR (Bio-Rad).[27] Relative mtDNA content was determined using ΔC_T method. Primers of the mtDNA encoded *CO1* gene were: forward, 5′-TGC TAGCCGCAGGCATTAC-3′; reverse, 5′-GGGTGCCCAAAGAATCA GAAC-3′. Primers of the single-copy nuclear gene *Ndufv1* were: forward, 5′-CTTCCCCACTGGCCTCAAG-3′; reverse, 5′-CCAAAACC CAGTGATCCAGC-3′.

2.8 ROS measurements

MitoSOX Red (Invitrogen) was used to measure mitochondrial reactive oxygen species (ROS) production. Isolated cardiomyocytes were loaded with MitoSOX Red (3 mM) in Dulbecco's Modified Eagle's Medium (DMEM) for 20 min at room temperature, followed by wash out. Images were obtained of cardiomyocytes by use of fluorescence microscopes (excitation at 514 nm and measuring the emitted light at 585 nm).

2.9 Intracellular ATP measurement

Heart tissue was collected from sham operations or *in vivo* regional ischaemia 45 min and reperfusion 24 h. The tissue was used to measure the intracellular ATP levels were measured using ATP Assay kit (Sigma MAK190-1KT) according to the manufacturer's instructions.

2.10 SIRT1 activity measurement

SIRT1 deacetylase activity assays were performed with the Fluor de Lys SIRT1 Fluorescent Activity Assay/Drug Discovery Kit (Enzo Life Sciences, Farmingdale, NY) according to the manufacturer's instructions. Fluorescent intensity was measured using a Bio-Tek Multifunction Plate Reader (BioTek Instruments, Winooski, VT). SIRT1 activity was calculated with the corrected arbitrary fluorescence units of the tested samples to no-enzyme control and expressed as fluorescent units relative to the control.

2.11 Transmission electron microscope

Heart tissues were rapidly immersed in tissue fixative buffer (10% formaldehyde, buffered, pH 7.4, Carson–Millonig formulation; RI31911; Ricca Chemicals, Arlington, TX) at 4°C for at least 8 h. Fixed tissues were trimmed to 1 mm^3 in size, stained with OsO_4 for 1 h, dehydrated in a graded ethanol series for 10 min per step (once in 35%, 50%, 70%, and 95% and twice in 100% ethanol), washed twice with acetone for 15 min per wash, washed in a solution of 1:1 acetone: Epon for 1 h, and finally embedded in 100% Epon (Ted Pella, Redding, CA) for 30 min. After incubating at 60°C overnight, the Epon block was semithin sectioned (10–12 1-μm-thick sections) by using Sorvall MT-6000-XL (RMC Boeckeler, Tucson, AZ) and a glass knife. Semithin sections were stained with 1% toluidine and observed under a light microscope to locate interested areas for ultrathin sections. After trim, the Epon block was thin sectioned (70 nm thick) by using a Leica Reichert Ultracut microtome and diamond knife. Thin sections were then applied on copper grids, air dried, stained with 2% uranyl acetate for 3 min and calcinated lead citrate for 30 s, and rinsed in distilled water by briskly dipping up and down for 20 s. The stained grid was loaded in a Jem1400 transmission electron microscopy (Jeol, Tokyo, Japan) with an ANT camera system located in the Department of Pathology, University of Mississippi Medical Center. At least 5 sections from each sample were examined under transmission electron microscope. Each entire section was thoroughly viewed at low magnifications to find areas of interest and to observe size, shape, and arrangement of subcellular organelles, including mitochondria, lipid droplets, nuclei, chromatin, and muscle fibers.[28]

2.12 Mitochondrial image analysis

Image analysis was performed using NIH Image J for mitochondrial size and relative abundance. The latter was calculated by fraction of mitochondria area/cell area.

2.13 Isolated heart perfusions

Mice were anesthetized with isoflurane (1–3%) and the isolated mouse hearts were perfused in the Langendorff mode with modified Krebs–Henseleit buffer containing glucose (7 mM), oleate (0.4 mM), BSA (1%), and a low fasting concentration of insulin (10 μU/mL) at 37°C, as previously described.[24,25] Hearts were perfused for 20 min at a flow of 4 mL/min, followed by 20 min of global, no-flow ischaemia and 30 min of reperfusion. A fluid-inflated balloon connected to Chart7 system from ADInstruments was inserted into the left ventricle (LV) to measure heart rate and left ventricular developed pressure (LVDP). The balloon was filled to achieve a baseline LV end-diastolic pressure of 5 mm Hg that was kept constant during ischaemia and reperfusion.[2,24,26]

2.14 Cell surface GLUT4 labelling

To distinguish cell surface and intracellular GLUT4, the cell membrane impermeable compound 4,4′-O-[2-[2-[2-[2-[2-[6(biotinylamino)-hexanoyl]-amino]ethoxy]-ethoxy]-ethoxy]-4-(1-azi-2,2,2,-trifluoroethyl)-benzyol]-amino-1.3-propanediyl] bis-D-glucose (bio-LC-ATB-BGPA) was used as previously described.[29,30] After perfusion in Langendorff system, isolated hearts were flushed with 1 mL of cold glucose-free KHB through aortic cannulation to wash away glucose and then perfused with KHB containing 300 μM of bio-LC-ATB-BGPA. After infusing with bio-LC-ATB-BGPA the hearts were incubated at 4°C for 15 min. In order to enhance the crosslink of GLUT4 and bio-LC-ATB-BGPA, the left and right ventricles were then cut sagittally and exposed under UV irradiation on both sides for 5 min each. Hearts were then freeze-clamped and stored in -80°C for further use. For cell surface GLUT4 analysis, the photolabelled cardiac tissues were homogenized in 500 μL lysis buffer containing 250 μL HEPES-EDTA-sucrose (HES) buffer (20 mM HEPES, 5 mM Na-EDTA, and 255 mM sucrose), 250 μL of 2% Thesit/PBS, and protease inhibitor cocktail (Hoffmann-La Roche Inc., Indianapolis, IN). Tissue homogenates were centrifuged at 20 000 *g*, 4°C for 30 min, and the supernatant was collected. To isolate the cell surface GLUT4, 400 μg of total protein were incubated with 100 μL of streptavidin bound to 6% agarose beads (Pierce, Rackford, IL) at 4°C overnight. The streptavidin-agarose isolated fraction of GLUT4 was then washed with decreasing concentrations of Thesit/PBS (1%, 0.1%, and 0%) three times. The labelled GLUT4 were then dissociated from the streptavidin by boiling in the LDS–PAGE loading buffer (Invitrogen) for 30 min. Western blot was conducted to compare the change of cell surface GLUT4.

2.15 Glucose uptake and glycolysis analysis

Glucose uptake and glycolysis were processed in two different experiments. Glucose uptake or glycolysis was analysed in the Langendorff heart perfusion system by measuring the production of ^3H_2O from D-[2-^{3}H]-glucose or D-[5-^{3}H]-glucose, respectively. Mice were heparinized (100 units i.p.) 10 min before being anesthetized. Isolated hearts were then retroperfused in the Langendorff perfusion system (Radnoti, Monrovia, CA) with Krebs–Henseleit buffer (KHB) containing 7 mM glucose, 1% BSA, 0.4 mM sodium oleate, 10 μU/mL insulin, and D-[2-^{3}H]-glucose/D-[5-^{3}H]-glucose bubbled with 95% O_2/5% CO_2. The whole system was kept at 37°C. For both glucose uptake and glycolysis measurements, isolated hearts were subjected to 20 min basal perfusion, followed by 10 min global, non-flow ischaemia and then 20-min reperfusion. Perfusate was recycled and collected every 5 min to test the radioactivity. Metabolized ^3H_2O was separated from D-[2-^{3}H]-glucose or D-[5-^{3}H]-glucose by filtering through an anion exchange 1-X8 resin (Bio-Rad, Hercules, CA). The rate of glucose uptake and glycolysis were calculated by the amount of ^3H_2O production. About 10 mL of scintillation fluid was added to each *vial* and then mixed well. The radioactive signal was measured on a liquid scintillation counter.

2.16 Fatty acid/glucose oxidation analysis

The working heart preload was set up at 15 cm H_2O, and the afterload was set at 80 cm H_2O.[19,25,31] The flow rate was kept at 15 mL/min. Aortic systolic and diastolic pressure (mmHg) were measured using a pressure transducer connected to aortic outflow line. Cardiac output and coronary flow (cardiac output minus aortic flow) were measured using in-line ultrasonic flow probes connected to a Transonic T402 ultrasonic flow meter. [9,10]-^{3}H-oleate (50 μci/L) and ^{14}C-glucose (20 μci/L) labelled BSA buffer was perfused into the heart through the pulmonary vein and pumped out through the aorta. The perfusate pumped out from the aorta and that outflowed from the coronary venous was recycled and collected every 5 min to test the radioactivity. The fatty acid level was determined by the production of ^3H_2O from [9,10]-^{3}H-oleate. Metabolized ^3H_2O was separated from [9,10]-^{3}H-oleate by filtering through an anion exchange resin (BioRad, Hercules, CA). Glucose oxidation was measured by metabolized $^{14}CO_2$ desolved in buffer or gaseous (further solved in sodium hydroxide and sampled every 5 min). To separate $^{14}CO_2$ from ^{14}C-glucose, sulfuric acid was added into perfusate samples to release $^{14}CO_2$. The ^{3}H and ^{14}C signals were detected to discriminate metabolic products from fatty acid and glucose, respectively.

2.17 Statistical analysis

Data were collected from experimental animals and presented as means ± SEM, as indicated, using Image GraphPad Prism 5.0 software (GraphPad Software, La Jolla, CA) for analysis. Comparisons were performed using either a two-tailed, unpaired Student's *t* test, Mann–Whitney *U* test, or ANOVA using Tukey's post-test, when appropriate. $P < 0.05$ was considered significant.

3. Results

3.1 Cardiomyocyte SIRT1 deficiency increased susceptibility to ischemic and reperfusion injury

We have reported that cardiac SIRT1 protein level and activity are declined in aging.[2] In order to explore the relationship between gene regulation by SIRT1 and gene regulation in response to ischaemia and reperfusion stress, we performed an expression microarray analysis upon inducible cardiac SIRT1 knockdown by tamoxifen (icSIRT1 KO) vs. SIRT1$^{flox/flox}$ hearts (*Figure 1A*). Total tested genes were 30854 by the beadchip (GPL22165). Depletion of cardiomyocyte SIRT1 significantly altered the gene expression profile, with approximately equal numbers of up- and down-regulated genes under both basal and ischaemia 45 min per reperfusion 24 h (I/R) conditions (using absolute log2-fold change of Illumina Mouse WG-6 v2.0 array average signal >5 as the significance criteria) (*Figure 1B*). These results suggest that cardiomyocyte SIRT1 is a key regulator of stress response genes in the heart.

In order to characterize the role of age-related SIRT1 decline in the heart's tolerance to ischemic insults, young WT (4–6 months), aged WT (24–26 months), and cardiomyocyte-specific SIRT1 knockout (icSIRT1 KO) C57BL/6 J mice were subjected to sham or ischaemia and reperfusion (I/R) operation. The echocardiography data demonstrated that

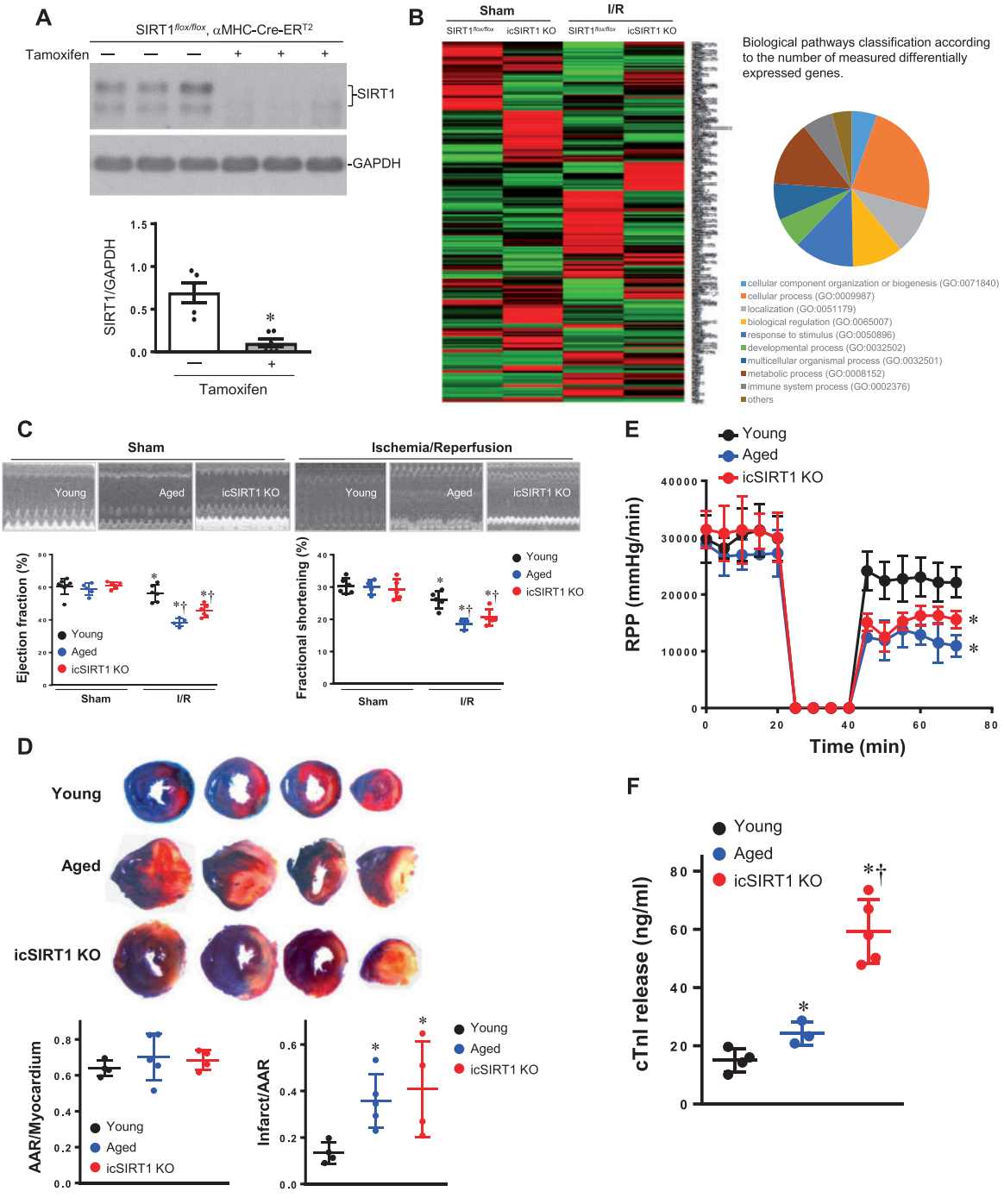

Figure 1 Inducible cardiomyocytes spcific SIRT1 knockout (icSIRT1 KO) mice. (*A*) Immunoblotting shows the down-regulation of heart SIRT1 after 10 days of Tamoxifen injection (0.08 mg/g, i.p. 5 days). $N = 6$, $^{*}P < 0.05$ using a Mann–Whitney *U* test between control and tamoxifen injection group. (*B*) Expression profile of heart under sham or ischaemia/reperfusion (I/R) condition in response to SIRT1 knockdown. The array was performed with an Illumina Mouse WG-6 v2.0 R2 expression beadchip (30854 genes), $n = 3$ for each group. (*C*) Echocardiography showed that ischaemia 45 min and reperfusion 24 h caused cardiac dysfunction in aged and icSIRT1 KO mice as shown by the decreased ejction fraction (EF) and fractional shortening (FS), $n = 5$–7, $^{*}P < 0.05$ vs. Sham, respectively; $^{\dagger}P < 0.05$ vs. young I/R using 2-way ANOVA with Tukey's post-test. (*D*) Young, aged, and icSIRT1 KO mice were subjected to *in vivo* regional ischaemia 45 min followed by 24-h reperfusion. Upper: representative sections of the extent of myocardial infarction; Lower left: ratio of the area at risk (AAR) to the total myocardial area; Lower right: ratio of the infarcted area (INF) to the area at risk (AAR). Values are means ± SEM, $n = 4$–5, $^{*}P < 0.05$ vs. young using 2-way ANOVA with Tukey's post-test. (*E*) Langendorff heart perfusion system showed a significant impaired post-ischemic recovery in aged and icSIRT1 KO hearts vs. young hearts, $n = 5$–6, $^{*}P < 0.05$ vs. young group, using 2-way ANOVA with Tukey's post-test. (*F*) Measurement of total cardiac troponin-I release in the serum from young, aged, and icSIRT1 KO mice at the end of reperfusion. Values are means ± SEM, $^{*}P < 0.05$ vs. young, $^{\dagger}P < 0.05$ vs. aged, $n = 4$–5 per group using 2-way ANOVA with Tukey's post-test.

there are no significant differences in contractile functions between young, aged, and icSIRT1 KO hearts (*Figure 1C* and see Supplementary material online, *Table S1*), but after ischaemia of 45 min by ligation of left anterior descending coronary artery (LAD) and reperfusion 24 h by release of LAD ligation, the aged and icSIRT1 KO mice demonstrated significantly impaired contractile functions such as ejection fraction (EF) and fractional shortening (FS) (*Figure 1C*). Moreover, the myocardial infarction size of aged and icSIRT1 KO hearts is significantly larger as compared to young hearts (*Figure 1D*). In order to determine the role of cardiac SIRT1 in cardiac function recovery during post-ischaemia, the isolated hearts from young, aged, or icSIRT1 KO mice were perfused in the Langendorff perfusion system. The results showed that after 20 min of global ischaemia followed by 30 min of reperfusion, the left ventricle contractility of aged and icSIRT1 KO hearts as shown by heart-rate-left-ventricular-developed pressure product (RPP) are significantly impaired as compared to that of young hearts (*Figure 1E*). There were no significant changes in heart rate between young, aged, and icSIRT1 KO hearts suggesting that the impairment in cardiac function after ischemic insults could not be ascribed to changes in chronotropic effects. Because ischaemia and reperfusion may cause myocardial stunning, where salvaged myocytes display a prolonged period of contractile dysfunction despite the absence of irreversible damage,[24] the question was then asked as to whether the impaired recovery of function in the aged and icSIRT1 KO hearts was due to either myocardial stunning or exacerbated cell death. As the amount of myocardial infarction correlates to the amount of cardiac-specific troponin-I released from cardomyocytes,[24,32,33] the amount of troponin-I release into the serum was measured and was found to be significantly elevated to the same degree as the extent of myocardial infarct size in the aged and icSIRT1 KO hearts vs. young hearts (*Figure 1F*).

3.2 SIRT1 deficiency impairs the AMPK signalling in ischemic heart

Accumulating evidence suggests that AMPK is a 'metabolic modulator', which can be an important effector of the switch between fatty acid and glucose oxidation during ischemic injury. We and others have shown that AMPK activation can improve the energetics during ischaemia, leading to rapid changes in fatty acid and glucose oxidation by increasing glucose uptake and rates of glycolysis and ATP generation.[31,34,35] There is evidence that cardiac SIRT1 also regulates substrate metabolism under normal physiological and stress conditions.[36] Thus, we hypothesized that SIRT1 might modulate AMPK activation, thereby promoting cardioprotection. Immunoblotting analysis of myocardial lysates taken from *in vivo* ischemic injury area demonstrated that ischaemia triggered AMPK phosphorylation in a time-dependent manner (*Figure 2A*), and the ischemic AMPK phosphorylation was impaired in the icSIRT1 KO hearts vs. $SIRT1^{flox/flox}$ littermate hearts (*Figure 2A*), especially at the 10-min time point of myocardial ischaemia (*Figure 2A*). The ability of AMPK to phosphorylate its immediate downstream target acetyl CoA carboxylase (ACC) was also significantly impaired in icSIRT1 KO hearts vs. $SIRT1^{flox/flox}$ littermate hearts in response to ischaemia (*Figure 2B*). Similarly, the aged WT and young WT hearts were subjected to 10 min of ischaemia by ligation of left anterior descending coronary artery. The immunoblotting of the ischemic region showed a significantly impaired phosphorylation of AMPK and downstream ACC in the aged WT vs. young WT hearts (*Figure 2C*). In order to understand the reason of an impaired ischemic AMPK activation occurring in aged WT and icSIRT1 KO hearts, the activation of AMPK upstream LKB1 was determined by immunoblotting with phosphorylation, acetylation, and ubiquitination-specific antibodies (*Figure 2D*); the results demonstrated that myocardial ischaemia stimulated phosphorylation of LKB1, and the ischemic LKB1 phosphorylation was impaired in icSIRT KO hearts (*Figure 2D*). Intriguingly, the immunoprecipitation data clearly showed that deacetylation of LKB1 occurring in young WT hearts but not in aged WT and young icSIRT1 KO hearts during myocardial ischaemia (*Figure 2D*). There was a strong ubiquitination modification of LKB1 in both aged WT and icSIRT1 KO hearts vs. young WT hearts (*Figure 2D*). These post-translational modifications of LKB1 could contribute to the impaired ischemic AMPK activation observed in aged WT and icSIRT1 KO hearts.

3.3 SIRT1 deficiency causes metabolic shift in response to ischemic stress

The *ex vivo* working heart system model was used to measure the substrate metabolism between young, aged, and icSIRT1 KO mouse hearts under basal perfusion and ischaemia and reperfusion stress conditions. D-[2-^{3}H]-glucose was used to measure glucose uptake.[26] The data showed that ischemic stress stimulated cardiac glucose uptake (*Figure 3A*), and the glucose uptake triggered by ischaemia and reperfusion was significantly blunted in aged and icSIRT1 KO hearts vs. young hearts (*Figure 3A*). D-[5-^{3}H]-glucose was used for glycolysis measurement.[30] Glucose oxidation was measured by the amount of [^{14}C] glucose metabolism into $^{14}CO_2$ in the *ex vivo* working hearts.[19] Fatty acid oxidation was measured by the incorporation of [9,10-^3H_2O] oleate into ^3H_2O.[19] The results demonstrated that ischaemia and reperfusion caused a significant metabolic shift between glucose metabolism and fatty acid oxidation in the heart (*Figure 3B–E*). Interestingly, both glycolysis and glucose oxidation were impaired in aged and icSIRT1 KO hearts vs. young hearts (*Figure 3B* and *C*), while the fatty acid oxidation was significantly augmented in aged and icSIRT1 KO hearts vs. young hearts during ischaemia and reperfusion (I/R) (*Figure 3D* and *E*). The cardiac pumping ability measured in working heart perfusion system is shown in Supplementary material online, *Table S2*; there is no significant change of cardiac pumping functions between young, aged, and icSIRT1 KO hearts under basal and ischemic stress conditions (see Supplementary material online, *Table S2*). However, the diastolic pressure of aged and icSIRT1 KO hearts was significantly higher than that of young hearts (see Supplementary material online, *Table S2*).

3.4 SIRT1 deficiency sensitizes mitochondria to ischemic insults

In order to determine the effect of an impaired energy sensor AMPK signalling on mitochondria structure and physiological functions, the transmission electron microscope was used to observe the morphology of mitochondria in young, aged, and icSIRT1 KO hearts. The results showed that mitochondria fission occurred in aged and icSIRT1 KO hearts as compared to young hearts (*Figure 4A* and *C*). Moreover, the mitochondria in both aged and icSIRT1 KO hearts demonstrated an increased sensitivity to ischaemia and reperfusion stress than that of young hearts, i.e. there are less density of mitochondria in aged and icSIRT1 KO hearts vs. young hearts during ischaemia and reperfusion (*Figure 4B*). The quantitative analysis of mitochondrial DNA (mtDNA) showed more damages occurred in aged and icSIRT1 KO heart mitochondria vs. young heart mitochondria during ischaemia and reperfusion (*Figure 4D*). The alterations could be associated with the impaired cardioprotective signalling pathways such as AMPK, extracellular-regulated protein kinase (ERK) autophagic flux occurred in aged and icSIRT1 KO hearts in response to

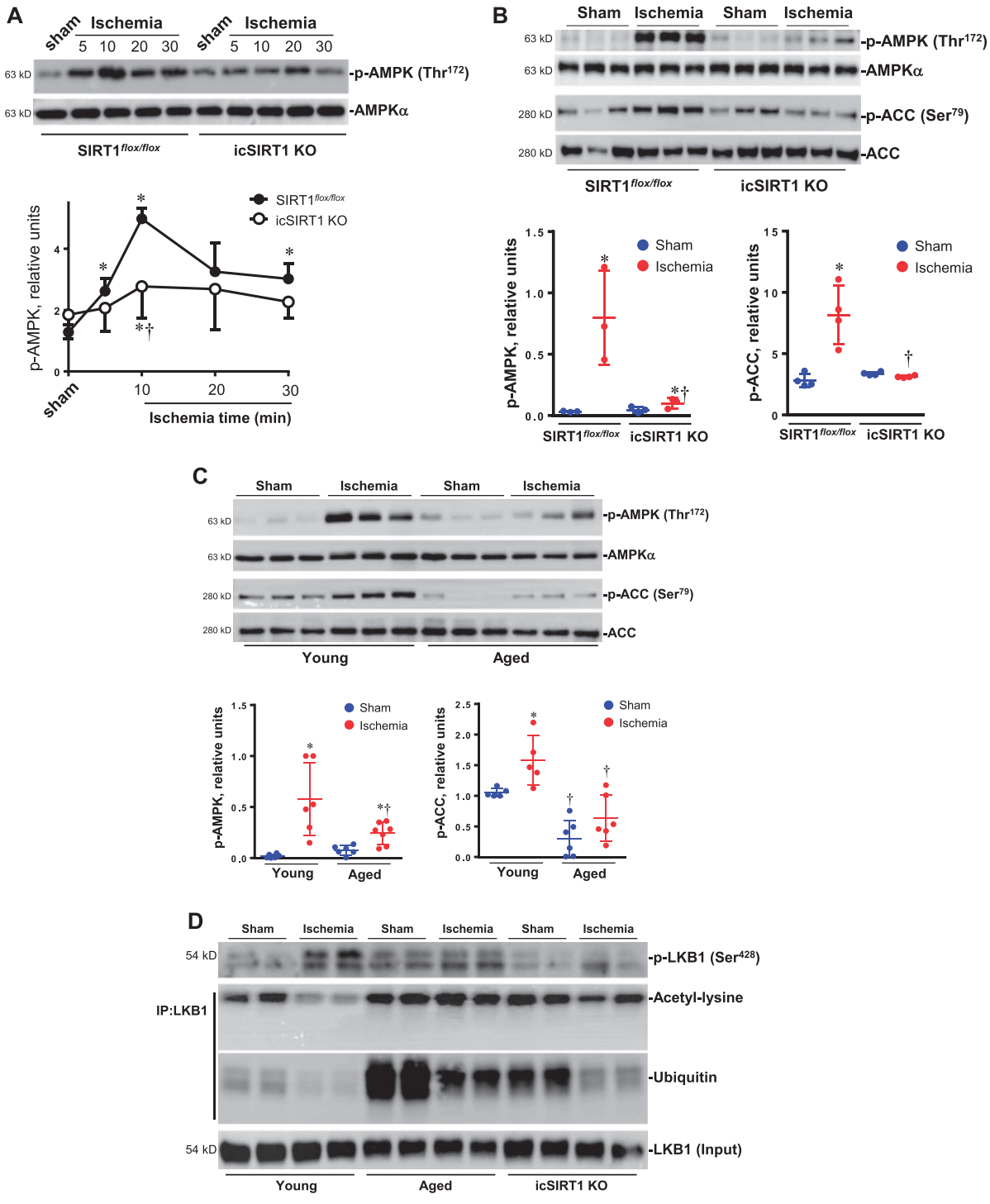

Figure 2 Impaired ischemic AMPK activation in aged and icSIRT1 KO hearts. (*A*) Immunoblotting measured the phosphorylation level of AMPK of ischemic region in response to different time points of myocardial ischaemia in young SIRT1$^{flox/flox}$ and young icSIRT1 KO hearts. Values are means ± SEM, $n = 4$, $^{*}P < 0.05$ vs. sham, respectively; $^{\dagger}P < 0.05$ vs. SIRT1$^{flox/flox}$ ischaemia using 2-way ANOVA with Tukey's post-test. (*B*) Immunoblotting of phosphorylation level of AMPK and AMPK downstream acetyl CoA carboxylase (ACC) in SIRT1$^{flox/flox}$ and icSIRT1 KO hearts under sham or 10 min of ischaemia. Values are means ± SEM, $n = 3$–4, $^{*}P < 0.05$ vs. sham, respectively; $^{\dagger}P < 0.05$ vs. SIRT1$^{flox/flox}$ ischaemia using 2-way ANOVA with Tukey's post-test. (*C*) Immunoblotting of phosphorylation level of AMPK and AMPK downstream ACC in the ischemic region of young and aged hearts under sham or 10 min of ischaemia. Values are means ± SEM, $n = 4$–6, $^{*}P < 0.05$ vs. sham, respectively; $^{\dagger}P < 0.05$ vs. young ischaemia using 2-way ANOVA with Tukey's post-test. (*D*) Immunoblotting showed the phosphorylation levels of AMPK upstream kinase LKB1 in the ischemic region of young, aged, and icSIRT1 KO hearts under sham or ischaemia conditions, the immunoprecipitation of LKB1 were used for assessing acetylation and ubiquitination levels of LKB1 occurred in young, aged, and icSIRT1 KO hearts as shown by the immunoblotting with antibodies recognized acetyl-lysine and ubiquitin, respectively.

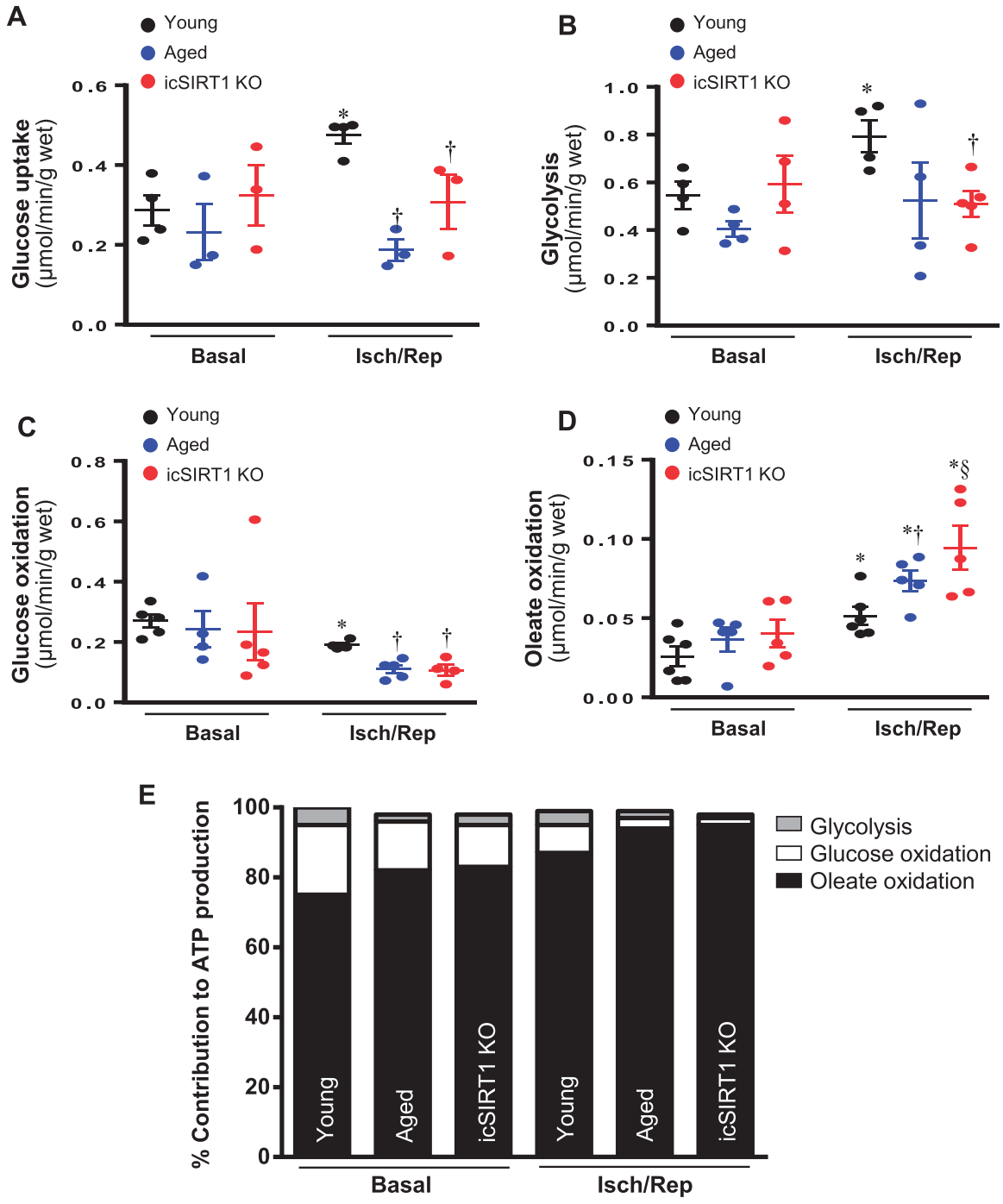

Figure 3 The mismatch substrate metabolism occurred in aged and icSIRT1 KO hearts. (*A*) D-[2-^{3}H]-glucose were used for determining the glucose uptake in young, aged, and icSIRT1 KO hearts under basal or ischaemia/reperfusion conditions. Values are means ± SEM, $n = 3$–4, $^{*}P < 0.05$ vs. basal, respectively; $^{\dagger}P < 0.05$ vs. young I/R using 2-way ANOVA with Tukey's post-test. (*B*) D-[5-^{3}H]-glucose were used in the heart perfusion system to measure glycolysis rate in young, aged, and icSIRT1 KO hearts under basal or ischaemia/reperfusion conditions. Values are means ± SEM, $n = 4$–5, $^{*}P < 0.05$ vs. basal, respectively; $^{\dagger}P < 0.05$ vs. young I/R using 2-way ANOVA with Tukey's post-test. (*C*) Glucose oxidation and (*D*) Oleate oxidation in the isolated working heart perfusion system. After balancing 20 min, isolated hearts were subjected to 10 min of ischaemia and 20 min of reperfusion. Glucose oxidation was analysed by measuring [^{14}C] glucose metabolism into $^{14}CO_2$. Oleate oxidation was measured by the incorporation of [9,10-$^{3}H_2O$] oleate into $^{3}H_2O$. Values are means ± SEM, $n = 4$–6, $^{*}P < 0.05$ vs. basal, respectively; $^{\dagger}P < 0.05$ vs. young I/R; $^{\S}P < 0.05$ vs. aged I/R using 2-way ANOVA with Tukey's post-test. (*E*) Relative percentage of ATP production from glucose and oleate oxidation in young, aged, and icSIRT1 KO hearts.

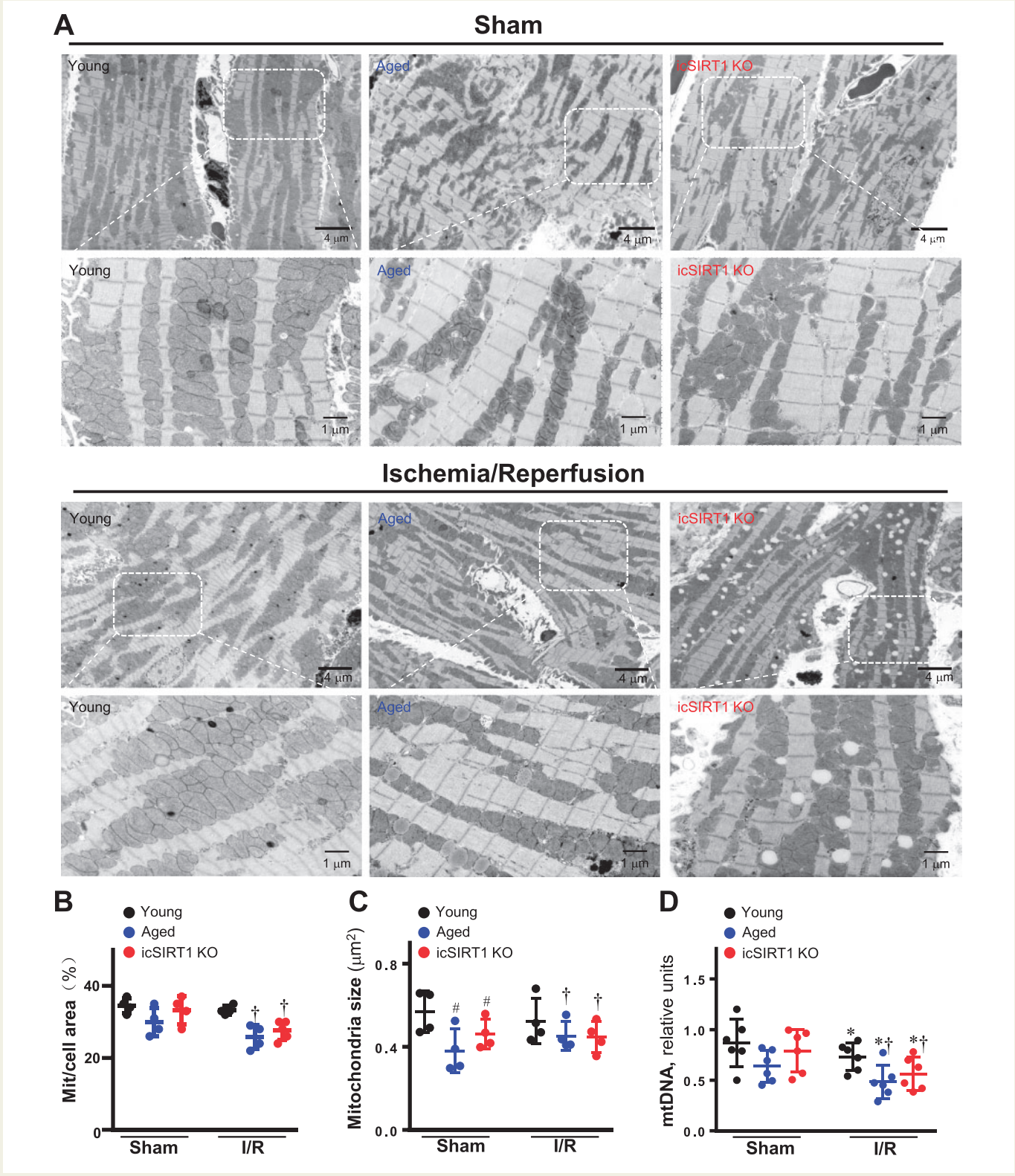

Figure 4 Mitochondrial alterations with aging sesitize heart to ischemic insults. (*A*) Transmission electronic microcope showed mitochondria morphology of young WT, aged WT, and young icSIRT1 KO hearts under sham operations or ischaemia 45′/reperfusion 24 h conditions. Quantitative analysis of relative abundance of mitochondria (calculated by mitochondria area/cell area) (*B*) and mitochondria size (*C*). Values are means ± SEM, $n = 4$ per group, $^{*}P < 0.05$ vs. sham, respectively; $^{\#}P < 0.05$ vs. young Sham; and $^{\dagger}P < 0.05$ vs. young I/R using 2-way ANOVA with Tukey's post-test. (*D*) Real-time–PCR measured the relative mitochondrial DNA (mtDNA) content (normalized to the single-copy nuclear gene Ndufv1) in heart tissue of young, aged, and icSIRT1 KO hearts. Values are means ± SEM, $n = 6$, $^{*}P < 0.05$ vs. sham, respectively; $^{\dagger}P < 0.05$ vs. young I/R using 2-way ANOVA with Tukey's post-test.

ischaemia and reperfusion stress (*Figure 5A*). The immunoblotting data of AMPK and downstream ACC and Raptor demonstrated that there is an impaired AMPK signalling response in aged and icSIRT1 KO hearts vs. young hearts (*Figure 5A*). The phosphorylation of autophagy-related kinase ULK1 demonstrated that there were impaired autophagic influx in aged and icSIRT1 KO hearts vs. young hearts during ischaemia and reperfusion (*Figure 5A*). Intriguingly, ischemic insults stimulated the up-regulation of the mitochondrial membrane protein UCP1 and mitochondrial pro-apoptotic protein BNIP3 (*Figure 5A*). The up-regulation of UCP1 and BNIP3 are augmented in aged and icSIRT1 KO hearts (*Figure 5A*). The mitochondria biogenesis-related protein PGC-1α that is regulated by AMPK[37] and SIRT1[38] was down-regulated in aged and icSIRT1 KO hearts as compared to young hearts (*Figure 5A*, the 2nd band from bottom). Moreover, ischaemia and reperfusion also triggers phosphorylation of inflammation signalling c-Jun N-terminal protein kinase (JNK) and oxidative stress marker 4-HNE (*Figure 5A*). The impaired AMPK and ERK signalling and autophagy regulation in aged and icSIRT1 KO hearts vs. young hearts during ischaemia and reperfusion, may affect mitochondria functions and cause oxidative stress, as shown by more 4-HNE adduct products in aged and icSIRT1 KO hearts vs. young hearts during ischaemia and reperfusion (*Figures 4* and *5*). The reactive oxygen species (ROS) levels from aged and icSIRT1 cardiomyocytes under hypoxia and reoxygenation conditions were higher than young cardiomyocytes (*Figure 5B*). Furthermore, the intracellular ATP generations were impaired in aged and icSRT1 KO hearts vs. young hearts in response to ischaemia and reperfusion stress (*Figure 5C*).

3.5 LKB1 hyper-acetylation blocks ischemic AMPK activation in the heart

In order to characterize the role of acetylation of LKB1 in ischemic AMPK activation in the hearts, SIRT1$^{flox/flox}$ and icSIRT1 KO mice were subjected to sham or ligation of left anterior descending coronary artery (LAD) operations with different time points. The myocardial lysates of the ischaemia region were immunoprecipitated by LKB1 antibody and the immunoblotting with antibody of acetyl-lysine showed that ischaemia triggered LKB1 deacetylation in SIRT1$^{flox/flox}$ hearts but not in icSIRT1 KO hearts (*Figure 6A*). The immunoprecipitation of a scaffold protein of AMPK, Sestrin2, demonstrated that the association between Sestrin2 and AMPK was abolished in the icSIRT1 KO vs. SIRT1$^{flox/flox}$ hearts (*Figure 6B*), and the interaction between Sestrin2 and AMPK upstream kinase LKB1 was also diminished in the icSIRT1 KO vs. SIRT1$^{flox/flox}$ hearts (*Figure 6B*). These data suggest that ischaemia stimulate SIRT1 activation that deacetylate LKB1 to increase the interaction between Sestrin2-AMPK complex and LKB1 in SIRT1$^{flox/flox}$ hearts, but this action is abolished in icSIRT1 KO hearts due to lack of SIRT1 activity.

Using BGPA photolabelling to determine the amount of glucose transporter GLUT4 on the cell surface,[26] the data showed that one of downstream AMPK action GLUT4 translocation triggered by ischaemia was significantly impaired in icSIRT1 KO vs. SIRT1$^{flox/flox}$ hearts (*Figure 6C*). The immunoprecipitation of GLUT4 data demonstrated that ischaemia stimulated a disassociation between GLUT4 and a GLUT4 anchor protein TUG (Tether containing UBX domain for GLUT4) in SIRT1$^{flox/flox}$ hearts, while ischaemia seems to enhance the interaction between TUG and GLUT4 in icSIRT1 KO hearts (*Figure 6D*). Furthermore, icSIRT1 KO hearts showed more sensitivity to ischemic insults as shown by more serum troponin release, higher oxidative stress level (p-Shc[66]), and impaired autophagic influx (p-eEF2, p-ULK1, LC3II/LC3I, and p62) vs. SIRT1$^{flox/flox}$ hearts (*Figure 6E*). Cardiac SIRT1 deficiency also increases acetylation of p65 of NF-κB that attenuates an adaptive acute response phosphorylation of p65 by ischemic stress (*Figure 6E*, the 8th and 9th bands). Therefore, the pro-apoptotic markers such as BNIP3 and Bax were up-regulated while anti-apoptotic proteins such as Bcl-2 and Bcl-xL got down-regulated during ischemic stress in icSIRT1 KO vs. SIRT1$^{flox/flox}$ hearts (*Figure 6E*).

3.6 Rescue of impaired SIRT1 level in aged heart improve tolerance of aged heart

In order to assess the contributions of SIRT1 to the impaired cardiac functions in aged hearts during ischaemia and reperfusion stress conditions, the adeno-associated virus (AAV9) was injected into the left ventricular cavity through a 27-G catheter while the aorta and pulmonary artery were crossed-clamped for 50 s. This procedure allows the solution that contains the adeno-associated virus (AAV9) to circulate down the coronary arteries and perfuse the heart without direct manipulation of the coronaries. After 7 days, the immunoblotting data showed that AAV9-Sirt1 rescues the levels of SIRT1 in the aged hearts (*Figure 7A*), and the impaired ischemic AMPK activation of aged vs. young hearts was rescued even higher than young hearts (*Figure 7B*). Importantly, the impaired cardiac functions of aged heart during ischaemia and reperfusion (I/R) are significantly improved with AAV9-Sirt1 treatment (*Figure 7C*); AAV9-Sirt1 treatment also significantly reduced the myocardial infarction size caused by ischaemia and reperfusion in the aged hears (*Figure 7D*). The glucose oxidation and oleate oxidation measurements in the *ex vivo* working hearts demonstrated that AAV9-Sirt1 treated aged hearts did not alter glucose oxidation in aged hearts (*Figure 7E*) but significantly attenuated the increased oleate oxidation occurring in the aged hearts during I/R (*Figure 7F* and *G*). The improvement of cardiac functions in the aged hearts by AAV9-Sirt1 could be associated with the increased ischemic AMPK activation in the aged hearts (*Figure 7A*) and the inhibition of fatty acid oxidation in the aged hearts during ischaemia and reperfusion (*Figure 7F* and *G*).

3.7 The relationship between AMPK signalling and SIRT1 activation in the heart

In order to define the relationship between AMPK signalling and SIRT1 activity in the heart in response to stress stimuli, FK866, an inhibitor of nicotinamide phosphoribosyltransferase (NAMPT),[39,40] was intravenously injected into mice to reduce intracellular NAD^+ level. The results demonstrated that FK866 treatment attenuated cardiac SIRT1 activation by ischaemia (*Figure 8A*). Interestingly, FK866 treatment significantly inhibited ischaemia-induced phosphorylation of AMPK and downstream acetyl CoA carboxylase (ACC) in the heart (*Figure 8C*). Moreover, AMPK kinase dead (AMPK KD) hearts showed significant lower SIRT1 activity vs. WT hearts in both sham and ischaemia conditions (*Figure 8B*). This data suggest that cardiac SIRT1 activity modulates AMPK signalling and AMPK activation also impact SIRT1 activity in the heart during normal physiological and stress conditions. Thus, there is a feedforward relationship between AMPK and SIRT1 in the heart.

In order to determine the feasibility of a pharmacological approach to improve the tolerance of aged hearts to ischemic insults, the isolated hearts from young and aged mice were perfused with AMPK agonist A769662 or SIRT1 agonist SRT1720 in the Langendorff system to measure glucose uptake and myocardial infarction during basal and ischaemia/reperfusion conditions. The results demonstrated that both A769662 and SRT1720 treatments can increase glucose uptake in young and aged hearts (*Figure 8D*), and A769662 treatment significantly reduce

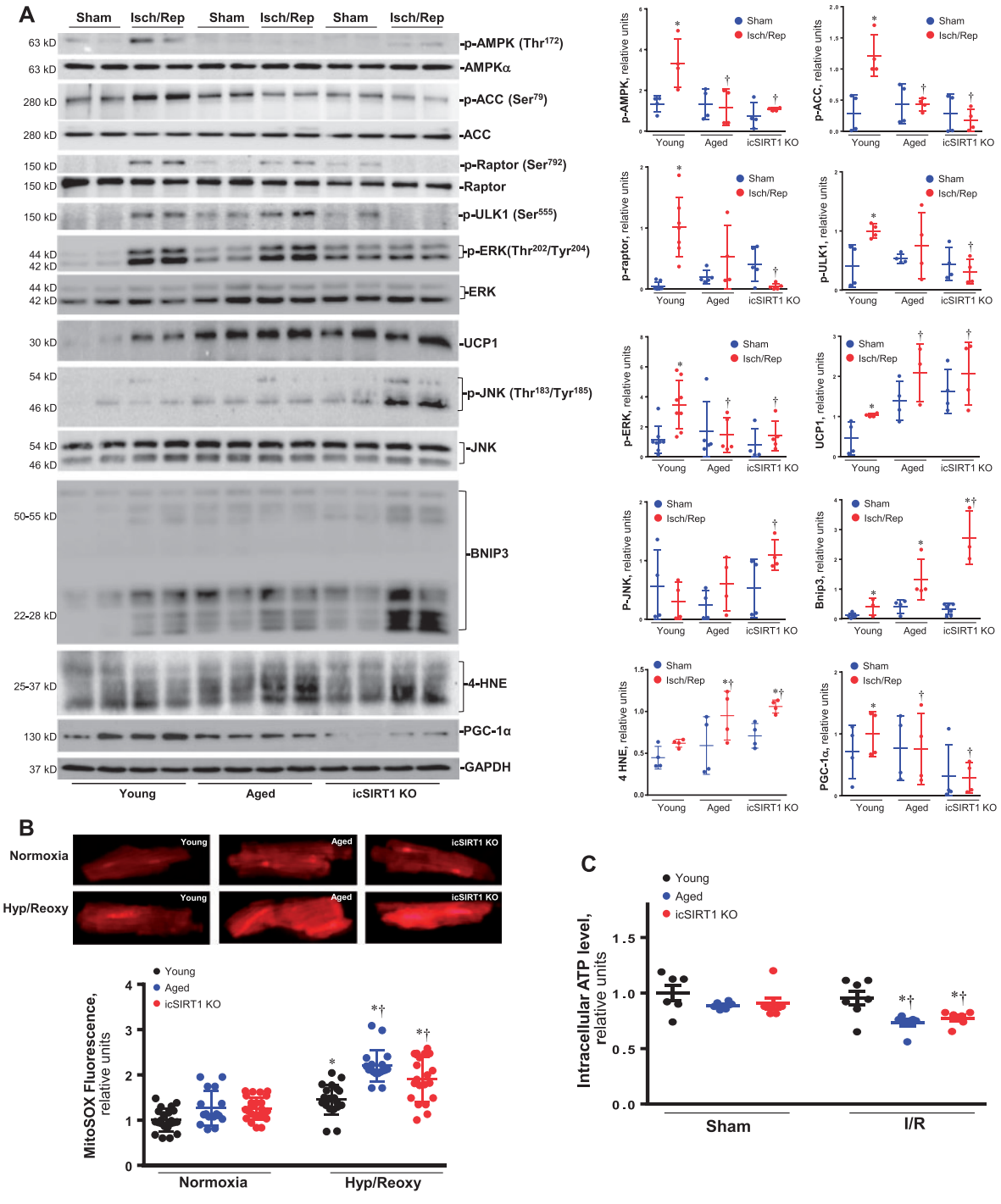

Figure 5 Autophagy signalling alterations with aging sesitize heart to ischemic insults. (*A*) Upper: immunoblots of phosphorylation of AMPK and downstream ACC, Raptor, and ULK1, phosphorlation of ERK and JNK, expression levels of mitochondrial membrane proteins UCP1, PGC-1α, and BNIP3, and oxidative stress marker 4-HNE in young, aged, and icSIRT1 KO hearts under sham operations or iscehmia 45′/reperfusion 24 h conditions to show the stress levels in the hearts; Lower: quantative analysis of relative levels of proteins in young, aged, and icSIRT1 KO hearts under sham or I/R conditions. The ratio phospho/total was normalized to GAPDH. Values are means ± SEM, $n = 4–8$, $^{*}P < 0.05$ vs. sham, respectively; $^{\dagger}P < 0.05$ vs. young I/R using 2-way ANOVA with Tukey's post-test. (*B*) Upper: representative images of reactive oxygen species (ROS) in cardiomyocytes from young, aged, and icSIRT1 KO hearts under normixa or hypoxia/reoxygenation conditions; Lower: quantitative analysis of the relative levels of ROS in young, aged, and icSIRT1 KO cardiomyocytes under normxia or hypoxia/reoxygenation conditions. Values are means ± SEM, $n = 15–20$, $^{*}P < 0.05$ vs. normoxia, respectively; $^{\dagger}P < 0.05$ vs. young hypoxia/reoxygenation using 2-way ANOVA with Tukey's post-test. (*C*) Relative intracellular ATP levels of young, aged, and icSIRT1 KO hearts under sham operations or ischaemia/reperfusion (I/R) conditions. Values are means ± SEM, $n = 6$, $^{*}P < 0.05$ vs. sham, respectively; $^{\dagger}P < 0.05$ vs. young I/R using 2-way ANOVA with Tukey's post-test.

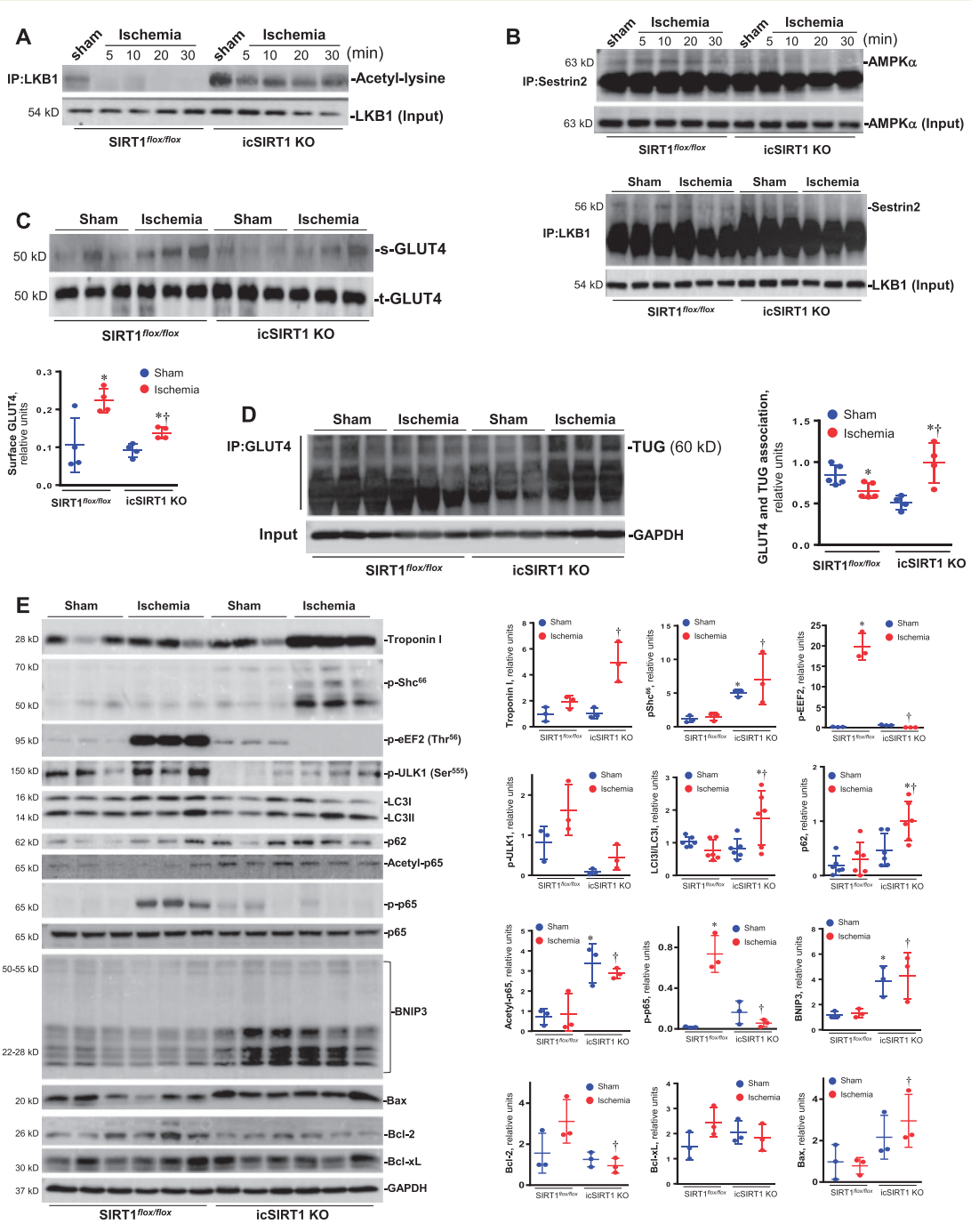

Figure 6 Hyper-acetylation of LKB1 attenuates AMPK signalling and GLUT4 translocation in icSIRT1 KO hearts. (*A*) The immunoblotting of immunoprecipitated LKB1 with antibody recognized acetyl-lysine showed that myocardial ischaemia triggered deacetylation of LKB1 in SIRT1$^{flox/flox}$ but not in icSIRT1 KO hearts. (*B*) The immunoprecipitation of a scaffold protein Sestrin2 showed the association between Sestrin2 and AMPKα was abolished in icSIRT1 KO hearts, LKB1 immunoprecipitation data also showed the diminished interaction between LKB1 and Sestrin2 in the icSIRT1 KO hearts vs. SIRT1$^{flox/flox}$ hearts. (*C*) Photolabelling with BGPA to measure the cell surface GLUT4 in SIRT1$^{flox/flox}$ and icSIRT1 KO hearts under sham or ischaemia conditions. Value are means ± SEM, $n = 4$ per group, $^{*}P < 0.05$ vs. sham, respectively, $^{\dagger}P < 0.05$ vs. WT ischaemia using 2-way ANOVA with Tukey's post-test. (*D*) The immunoprecipitation of GLUT4 showed a GLUT4 anchor protein TUG (Tether containing UBX domain for GLUT4) was dissociated with GLUT4 in the SIRT1$^{flox/flox}$ hearts in response to ischemic stress, while the interaction between GLUT4 and TUG was augmented in icSIRT1 KO hearts during ischaemia. Value are means ± SEM, $n = 4$–5 per group, $^{*}P < 0.05$ vs. sham, respectively; $^{\dagger}P < 0.05$ vs. SIRT1$^{flox/flox}$ ischaemia using 2-way ANOVA with Tukey's post-test. (*E*) Upper: The immunoblotting of cardiac damage marker Troponin I, oxidative stress marker Shc phosphorylation, autophagic influx proteins eEF2, ULK1, LC3II/LC3I, and p62, inflammation-related signalling p65 modifications, and mitochondrial proteins associated with apoptosis BNIP3, Bcl-2, Bcl-xL, and Bax, to show the sensitivity of SIRT1$^{flox/flox}$ and icSIRT1 KO hearts to ischemic stress; Lower: quantitative analysis of the relative levels of proteins in SIRT1$^{flox/flox}$ and icSIRT1 KO hearts under sham or ischaemia conditions. Values are means ± SEM, $n = 3$–6, $^{*}P < 0.05$ vs. sham, respectively; $^{\dagger}P < 0.05$ vs. SIRT1$^{flox/flox}$ ischaemia using 2-way ANOVA with Tukey's post-test.

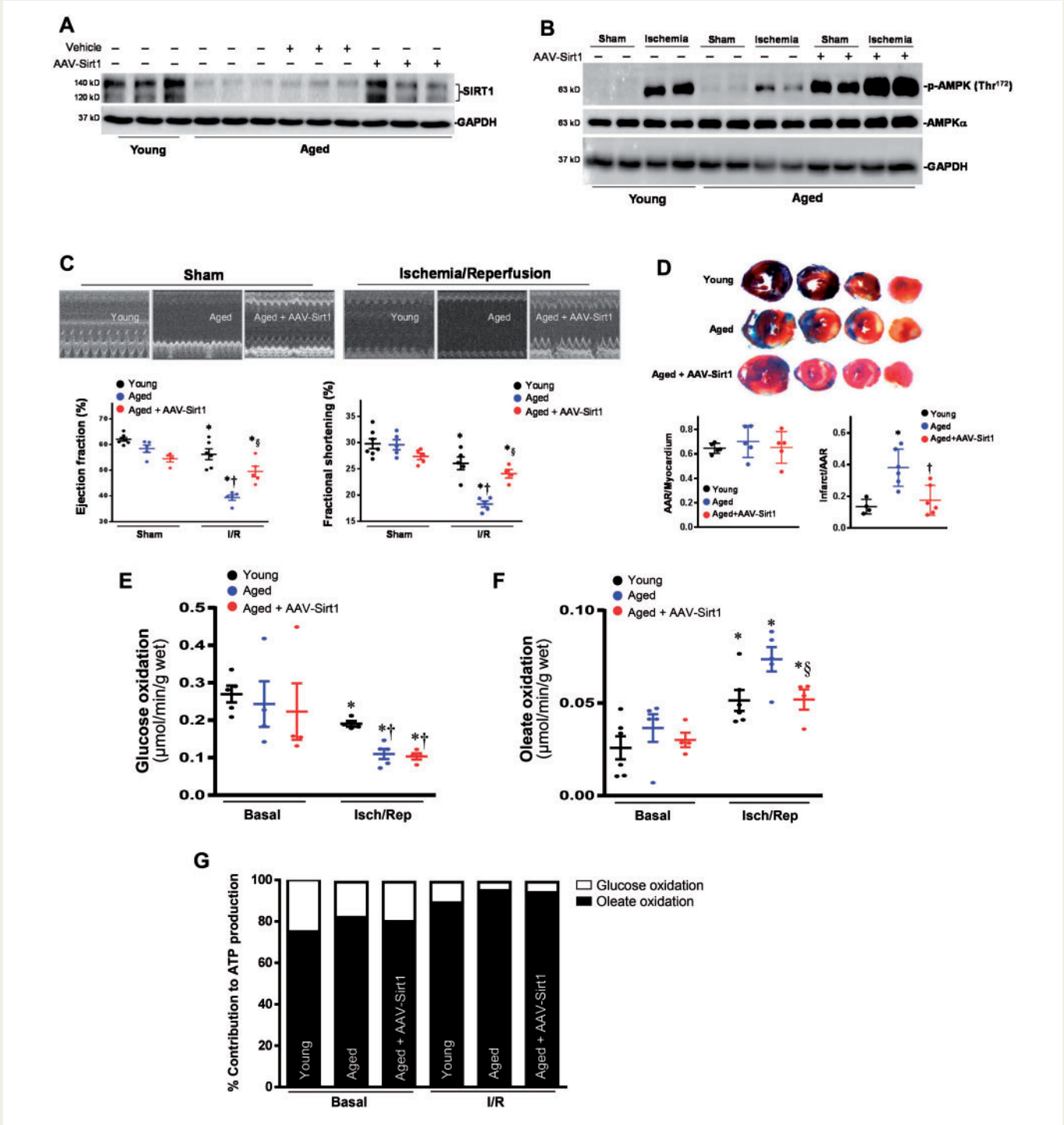

Figure 7 The recovery SIRT1 levels in aged hearts rescue AMPK signalling and resistance to ischemic stress. (*A*) Immunoblotting showed the recovery of SIRT1 expression levels in aged hearts by coronary delivery of AAV9-Sirt1. (*B*) Immunoblotting showed that the coronary delivery of AAV9-Sirt1 significantly rescues the ischmic AMPK phosphorylation in the aged hearts. (*C*) Echocardiography showed that recovery of impaired SIRT1 levels in the aged hearts improved the resistance of aged heart to ischemic stress as shown by ejection fraction (EF) and fractional shortening (FS). Values are means ± SEM, $n = 4–6$, $^{*}P < 0.05$ vs. Sham, respectively; $^{\dagger}P < 0.05$ vs. young I/R; $\S P < 0.05$ vs. aged I/R using 2-way ANOVA with Tukey's post-test. (*D*) Young, aged, and aged + AAV9-Sirt1 mice were subjected to *in vivo* regional ischaemia 45 min followed by 24-h reperfusion. Upper: representative sections of the extent of myocardial infarction; Lower left: ratio of the area at the risk (AAR) to the total myocardial area; Lower right: ratio of the infarcted area (INF) to AAR. Values are means ± SEM, $n = 5–6$, $^{*}P < 0.05$ vs. young, $^{\dagger}P < 0.05$ vs. aged using 2-way ANOVA with Tukey's post-test. (*E*) Glucose oxidation and (*F*) Oleate oxidation in the isolated working heart and (*G*) relative percentage of ATP production from glucose and oleate oxidation. After balancing 20 min, isolated hearts were subjected to 10 min of ischaemia and 20 min of reperfusion. Glucose oxidation was analysed by measuring [^{14}C] glucose metabolism into $^{14}CO_2$. Oleate oxidation was measured by the incorporation of [9,10-$^{3}H_2O$] oleate into $^{3}H_2O$. Values are means ± SEM, $n = 4–5$, $^{*}P < 0.05$ vs. basal, respectively; $^{\dagger}P < 0.05$ vs. young I/R; $\S P < 0.05$ vs. aged I/R using 2-way ANOVA with Tukey's post-test.

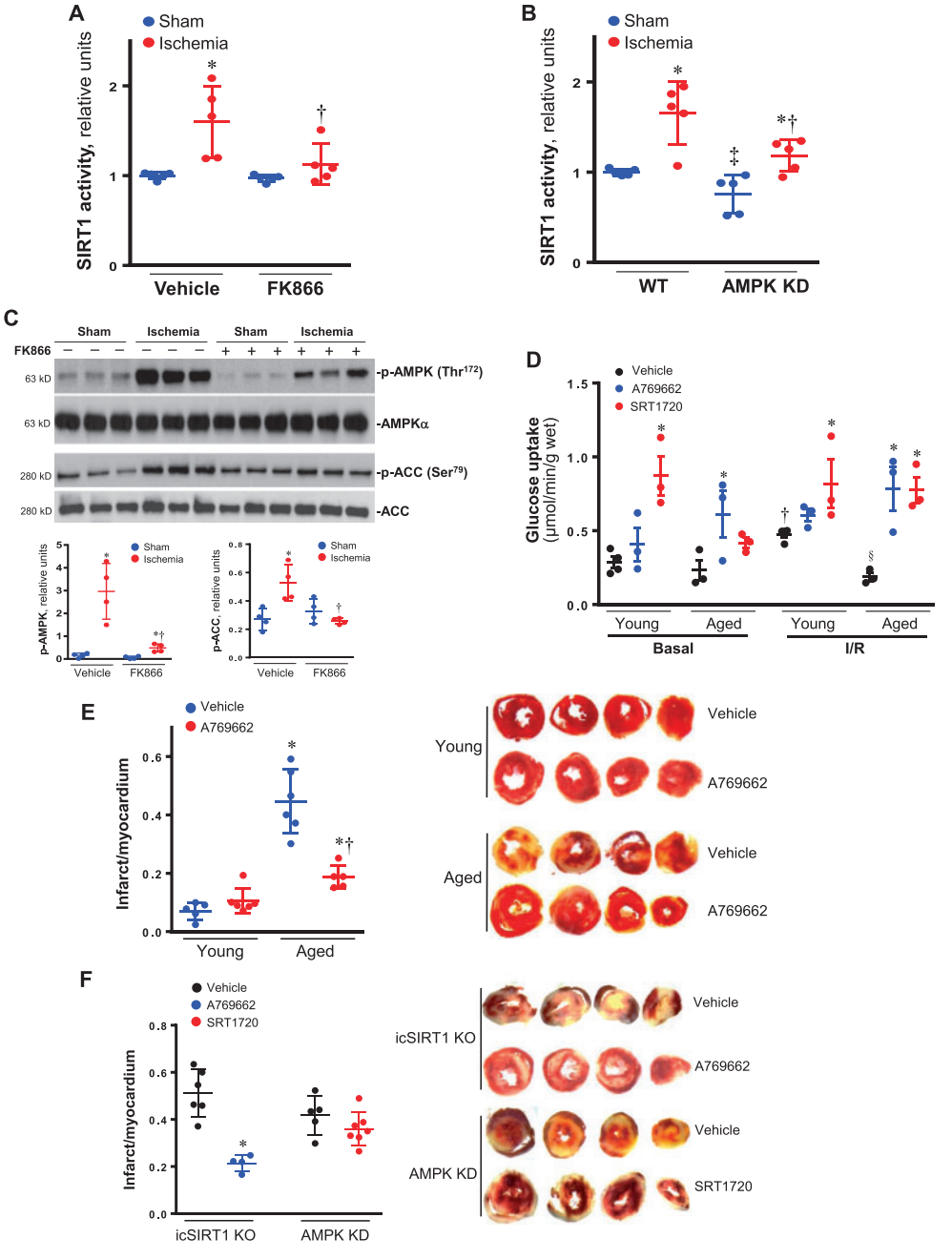

Figure 8 The feedforward relationship between AMPK and SIRT1 in the hearts. (*A*) The SIRT1 activity of hearts was measured with a commerical kit for vehicle or NAMPT inhibitor FK866 intravenously injection 4 h under sham operations or 10-min ischaemia conditions. Values are means ± SEM, $n = 5$, $^{*}P < 0.05$ vs. vehicle sham; $^{\dagger}P < 0.05$ vs. vehicle ischaemia using 2-way ANOVA with Tukey's post-test. (*B*) The cardiac SIRT1 activities were measured for WT littermates and AMPK kinase dead (AMPK KD) transgenic mice under sham operations or 10 min ischaemia conditions. Values are means ± SEM, $n = 5$, $^{*}P < 0.05$ vs. sham, respectively; $^{\dagger}P < 0.05$ vs. WT ischaemia; $^{\ddagger}P < 0.05$ vs. WT sham using 2-way ANOVA with Tukey's post-test. (*C*) Upper: the immunoblotting showed the inhibition of NAMPT inhibitor FK866 on phosphorylation of AMPK and downstream ACC induced by myocardial ischaemia. Lower: quantitative analysis of phosphorylation levels of AMPK and ACC. Values are means ± SEM, $n = 4$–5, $^{*}P < 0.05$ vs. vehicle sham, respectively; $^{\dagger}P < 0.05$ vs. vehicle ischaemia using 2-way ANOVA with Tukey's post-test. (*D*) D-[2-^{3}H]-glucose were used for determining the effect of AMPK agonist A769662 or SIRT1 agonist SRT1720 on glucose uptake in young and aged hearts under basal or ischaemia (10 min)/reperfusion (30 min) conditions. Values are means ± SEM, $n = 3$–4, $^{*}P < 0.05$ vs. vehicle, respectively; $^{\dagger}P < 0.05$ vs. basal, respectively; $^{\S}P < 0.05$ vs. young vehicle I/R using 2-way ANOVA with Tukey's post-test. (*E*) TTC staining shows the myocardial infarction in young and aged hearts after ischaemia/reperfusion with or without AMPK agonist A769662 in the heart perfusion system. Values are means ± SEM, $n = 5$–6, $^{*}P < 0.05$ vs. young group, respectively; $^{\dagger}P < 0.05$ vs. aged vehicle using 2-way ANOVA with Tukey's post-test. (*F*) TTC staining shows the myocardial infarction of icSIRT1 KO hearts after ischaemia/reperfusion with or without AMPK agonist A769662 in the heart perfusion system, and the myocardial infarction of AMPK KD hearts with or without SIRT1 agonist SRT1720 in the heart perfusion system. Values are means ± SEM, $n = 4$–6, $^{*}P < 0.05$ vs. icSIRT1 KO vehicle using 2-way ANOVA with Tukey's post-test.

myocardial infarction in the aged hearts caused by ischaemia and reperfusion (*Figure 8E*). In addition, AMPK agonist A769662 treatment significantly reduced myocardial infarction of icSIRT1 KO hearts (*Figure 8F*), while SIRT1 agonist SRT1720 did not significantly affect the myocardial infarction by ischaemia and reperfusion in AMPK KD hearts (*Figure 8F*). These data suggest that AMPK could be a good target for developing small molecules to improve the tolerance of aged hearts to ischemic insults.

4. Discussion

Our group and others have provided evidence that AMPK plays an important role in cardioprotection against ischaemia and reperfusion injury.[16,22,35,41–44] SIRT1 has emerged as a critical regulator during ischaemia/reperfusion in the heart.[2,45–48] Moreover, SIRT1 deacetylates AMPK upstream LKB1 leading to activation of AMPK, a central energy regulator involved in glucose homeostasis and maintenance of cellular ATP levels.[49] The functional AMPK is a heterotrimer consisting of a catalytic α, a regulatory γ, and a scaffolding β subunit and is activated by low cellular energy status.[50] AMPK activation orchestrates many biochemical events including glucose uptake, glycolysis, oxidation of free fatty acids, and mitochondrial biogenesis.[51] Our recent finding revealed a novel stress inducible protein Sestrin2 modulating cardiac AMPK to regulate glucose transporter trafficking.[52] AMPK also promotes autophagy and mitophagy, thus preventing mitochondrial insufficiency, inflammation, and cellular death.[53] Autophagy is a major intracellular degradation process recognized to play a central role in cell survival and longevity.[54] AMPK is also a master regulator of key molecular effectors involved in metabolic processes, longevity, and cardiovascular homeostasis. AMPK modulates mTOR signalling by directly phosphorylating the TSC1/2 complex, regulates the IGF-1 pathway, and controls SIRT activity by regulating the abundance of NAD and NAMPT activity.[50] Our results suggest that cardiac autophagy regulation by SIRT1-AMPK signalling cascades is impaired in aging. The impaired SIRT1-AMPK signalling by ischemic insults could cause mitochondria more susceptible to ischemic stress and trigger generation of reactive oxygen species that initiate inflammatory response during ischaemia and reperfusion. Interestingly, more evidence indicates that AMPK is amenable to pharmacological intervention and represents a potentially 'druggable' target to prevent ageing-related features. Metformin, a biguanide used in the treatment of diabetes, is capable of inducing AMPK activation. Administration of metformin before, during, or after myocardial ischaemia has been shown to prevent ischaemia–reperfusion injury and adverse remodelling of the left ventricle.[55] Metformin has been shown to preserve insulin secretion by promoting the AMPK-dependent autophagic response in pancreatic beta cells.[56]

SIRT1 belongs to the family of NAD-dependent proteins and is considered a major gatekeeper against oxidative stress, inflammation, and cardiovascular aging.[1] Cardiac SIRT1 activity is declined in senescence;[57] in fact, aged heart exhibited lower nuclear SIRT1 levels compared with those in young hearts, which was further down-regulated under ischaemia and reperfusion insult.[2] Activation of SIRT1 not only suppresses apoptosis but also balances oxidative stress in the heart, while absence of SIRT1 triggers chronic inflammation, oxidative stress, and cell cycle arrest.[58] SIRT1 acts as a cardioprotective molecule that protects from aging and induces resistance against hypertrophic and oxidative stresses, inhibits cardiomyocyte apoptosis, and regulates cardiac energy metabolism.[59] NAMPT is a critical determinant of the NAD^+ level in the heart at baseline and in response to stress.[60,61] Ischaemia/hypoxia injury demonstrated that the level of cellular NAD declined due to NAD^+-consuming poly (ADP-ribose) polymerase (PARP)-1 over-activation, mitochondrial permeability transition pore (mPTP) opening, and the down-regulation of NAMPT.[62] Down-regulation of Sirt1 caused accumulation of LC3-II and p62, thereby mimicking the effect of NAMPT down-regulation.[46] AMPK could enhance SIRT1 activity by increasing cellular NAD^+ levels.[6] Our results demonstrated that cardiac AMPK kinase dead transgenic mice attenuate cardiac SIRT1 activation in response to ischemic stress, and NAMPT antagonist FK866 also inhibits ischemic AMPK activation in the heart. Therefore, there is a feedforward relationship between AMPK and SIRT1 in the heart in response to ischemic insults.

LKB1 can be deacetylated by SIRT1. Such deacetylation in HEK293T cells correlates with increases in LKB1 activity, cytoplasmic localization and binding to STRAD, and AMPK and ACC phosphorylation.[10] Inflammation is a key mechanism for aging and age-related diseases, especially cardiovascular diseases.[63] SIRT1 was reported to negatively regulate the development and progression of inflammation. In this process, SIRT1 deacetylates the major transcription factors, NF-κB; this deacetylation results in the transcriptional inhibition of diverse inflammation-associated genes.[64] Our results clearly show that cardiomyocyte deletion of Sirt1 (icSIRT1 KO) causes hyper-acetylation of p65 of NF-κB and attenuates the phosphorylation of p65 by ischemic stress in the heart, consequently leading to more oxidative stress and apoptotic events occurred in icSIRT1 KO heart vs. $SIRT1^{flox/flox}$ heart during ischemic insults.

SIRT1-mediated inhibition of pShc[66] is an effective pathway for anti-oxidative stress and anti-aging. pShc[66] knockout mice have enhanced resistance to oxidative stress and a 30% increase in lifespan; pShc[66] augments reactive oxygen species (ROS)-dependent endothelial dysfunction induced by aging.[65,66] Therefore, endothelial function can be preserved and vascular aging can be delayed by inhibiting pShc.[66] SIRT1 negatively modulates pShc.[66,67] The results from icSIRT1 KO, aged, and young hearts demonstrated that cardiomyocytes SIRT1 deficiency in icSIRT1 KO and aged hearts cause more oxidative stress, as shown by higher level of 4-HNE and phosphorylation of pShc[66] vs. young hearts in response to ischemic insults. This study is the first examination of age-related protein SIRT1 in AMPK-mediated metabolic regulation during ischaemia and reperfusion stress conditions. Cardiomyocytes-specific SIRT1 knockout (icSIRT1 KO) mice and the aged mice demonstrated impaired AMPK signalling and higher fatty acid oxidation during ischaemia and reperfusion, by which more ROS could be generated from mitochondrial to damage the cells in the hearts.

The rescued SIRT1 in the aged hearts *via* AAV9 viral delivery significantly improved the tolerance of aged heart to ischemic insults as shown by echocardiography and myocardial infarction measurements. Interestingly, the viral delivery not only rescued the impaired ischemic AMPK activation but increased the basal levels of AMPK phosphorylation in the aged hearts as well. This could be due to more LKB1 deacetylation by the viral delivery of exogenous SIRT1 in the aged heart (data not shown). Furthermore, AMPK agonist attenuates cardiac damage by ischemic insults in the icSIRT1 KO hearts, but SIRT1 agonist does not show the beneficial effects on ischemic AMPK KD hearts.

In conclusion, the longevity protein SIRT1 modulates AMPK signalling pathway *via* deacetylation of AMPK upstream LKB1 in the heart during ischemic stress. Ischemic AMPK activation also regulates SIRT1 activity through modulating NAD level by NAMPT in the heart. There is a feedforward relationship between AMPK and SIRT1 in the heart in response

to ischemic insults, even though this feedforward relationship becomes weak with aging, pharmacological intervention with AMPK agonist or SIRT1 agonist could improve the tolerance of aged hearts to ischemic insults *via* modulating the cardiac AMPK signalling pathway.

Supplementary material

Supplementary material is available at *Cardiovascular Research* online.

Funding

These studies were supported by American Diabetes Association 1-17-IBS-296, NIH R21AG044820, R01AG049835, P30CA016056, P01HL051971, and P20GM104357.

Conflict of interest: none declared.

References

1. Pillarisetti S. A review of Sirt1 and Sirt1 modulators in cardiovascular and metabolic diseases. *Recent Pat Cardiovasc Drug Discov* 2008;**3**:156–164.
2. Tong C, Morrison A, Mattison S, Qian S, Bryniarski M, Rankin B, Wang J, Thomas DP, Li J. Impaired SIRT1 nucleocytoplasmic shuttling in the senescent heart during ischemic stress. *FASEB J* 2013;**27**:4332–4342.
3. Ali B, Parmar SS, Dwivedi C, Harbison RD. Selective inhibition of nicotinamide adenine dinucleotide dependent oxidations by substituted carbamides. *Res Commun Chem Pathol Pharmacol* 1975;**11**:163–166.
4. Alcendor RR, Gao S, Zhai P, Zablocki D, Holle E, Yu X, Tian B, Wagner T, Vatner SF, Sadoshima J. Sirt1 regulates aging and resistance to oxidative stress in the heart. *Circ Res* 2007;**100**:1512–1521.
5. Ruderman NB, Xu XJ, Nelson L, Cacicedo JM, Saha AK, Lan F, Ido Y. AMPK and SIRT1: a long-standing partnership? *Am J Physiol Endocrinol Metab* 2010;**298**: E751–E760.
6. Canto C, Gerhart-Hines Z, Feige JN, Lagouge M, Noriega L, Milne JC, Elliott PJ, Puigserver P, Auwerx J. AMPK regulates energy expenditure by modulating NAD+ metabolism and SIRT1 activity. *Nature* 2009;**458**:1056–1060.
7. Fulco M, Sartorelli V. Comparing and contrasting the roles of AMPK and SIRT1 in metabolic tissues. *Cell Cycle* 2008;**7**:3669–3679.
8. Ahmad F, Arad M, Musi N, He H, Wolf C, Branco D, Perez-Atayde AR, Stapleton D, Bali D, Xing Y, Tian R, Goodyear LJ, Berul CI, Ingwall JS, Seidman CE, Seidman JG. Increased alpha2 subunit-associated AMPK activity and PRKAG2 cardiomyopathy. *Circulation* 2005;**112**:3140–3148.
9. Costford SR, Kavaslar N, Ahituv N, Chaudhry SN, Schackwitz WS, Dent R, Pennacchio LA, McPherson R, Harper ME. Gain-of-function R225W mutation in human AMPKgamma(3) causing increased glycogen and decreased triglyceride in skeletal muscle. *PLoS One* 2007;**2**:e903.
10. Lan F, Cacicedo JM, Ruderman N, Ido Y. SIRT1 modulation of the acetylation status, cytosolic localization, and activity of LKB1. Possible role in AMP-activated protein kinase activation. *J Biol Chem* 2008;**283**:27628–27635.
11. Hou X, Xu S, Maitland-Toolan KA, Sato K, Jiang B, Ido Y, Lan F, Walsh K, Wierzbicki M, Verbeuren TJ, Cohen RA, Zang M. SIRT1 regulates hepatocyte lipid metabolism through activating AMP-activated protein kinase. *J Biol Chem* 2008;**283**:20015–20026.
12. Fulco M, Cen Y, Zhao P, Hoffman EP, McBurney MW, Sauve AA, Sartorelli V. Glucose restriction inhibits skeletal myoblast differentiation by activating SIRT1 through AMPK-mediated regulation of Nampt. *Dev Cell* 2008;**14**:661–673.
13. Scarpulla RC. Metabolic control of mitochondrial biogenesis through the PGC-1 family regulatory network. *Biochim Biophys Acta* 2011;**1813**:1269–1278.
14. Um JH, Park SJ, Kang H, Yang S, Foretz M, McBurney MW, Kim MK, Viollet B, Chung JH. AMP-activated protein kinase-deficient mice are resistant to the metabolic effects of resveratrol. *Diabetes* 2010;**59**:554–563.
15. Park SJ, Ahmad F, Philp A, Baar K, Williams T, Luo H, Ke H, Rehmann H, Taussig R, Brown AL, Kim MK, Beaven MA, Burgin AB, Manganiello V, Chung JH. Resveratrol ameliorates aging-related metabolic phenotypes by inhibiting cAMP phosphodiesterases. *Cell* 2012;**148**:421–433.
16. Ma H, Wang J, Thomas DP, Tong C, Leng L, Wang W, Merk M, Zierow S, Bernhagen J, Ren J, Bucala R, Li J. Impaired macrophage migration inhibitory factor (MIF)-AMPK activation and ischemic recovery in the senescent heart. *Circulation* 2010;**122**: 282–292.
17. Luptak I, Yan J, Cui L, Jain M, Liao R, Tian R. Long-term effects of increased glucose entry on mouse hearts during normal aging and ischemic stress. *Circulation* 2007;**116**: 901–909.
18. Desrois M, Sidell RJ, Gauguier D, Davey CL, Radda GK, Clarke K. Gender differences in hypertrophy, insulin resistance and ischemic injury in the aging type 2 diabetic rat heart. *J Mol Cell Cardiol* 2004;**37**:547–555.
19. Costa R, Morrison A, Wang J, Manithody C, Li J, Rezaie AR. Activated protein C modulates cardiac metabolism and augments autophagy in the ischemic heart. *J Thromb Haemost* 2012;**10**:1736–1744.
20. Mu J, Brozinick JT, Jr, Valladares O, Bucan M, Birnbaum MJ. A role for AMP-activated protein kinase in contraction- and hypoxia-regulated glucose transport in skeletal muscle. *Mol Cell* 2001;**7**:1085–1094.
21. Morrison A, Yan X, Tong C, Li J. Acute rosiglitazone treatment is cardioprotective against ischemia-reperfusion injury by modulating AMPK, Akt, and JNK signaling in nondiabetic mice. *Am J Physiol Heart Circ Physiol* 2011;**301**:H895–H902.
22. Wang J, Yang L, Rezaie AR, Li J. Activated protein C protects against myocardial ischemic/reperfusion injury through AMP-activated protein kinase signaling. *J Thromb Haemost* 2011;**9**:1308–1317.
23. Ommen SR, Nishimura RA, Appleton CP, Miller FA, Oh JK, Redfield MM, Tajik AJ. Clinical utility of Doppler echocardiography and tissue Doppler imaging in the estimation of left ventricular filling pressures: a comparative simultaneous Doppler-catheterization study. *Circulation* 2000;**102**:1788–1794.
24. Morrison A, Chen L, Wang J, Zhang M, Yang H, Ma Y, Budanov A, Lee JH, Karin M, Li J. Sestrin2 promotes LKB1-mediated AMPK activation in the ischemic heart. *FASEB J* 2015;**29**:408–417.
25. Yang H, Sun W, Quan N, Wang L, Chu D, Cates C, Liu Q, Zheng Y, Li J. Cardioprotective actions of Notch1 against myocardial infarction via LKB1-dependent AMPK signaling pathway. *Biochem Pharmacol* 2016;**108**:47–57.
26. Wang J, Tong C, Yan X, Yeung E, Gandavadi S, Hare AA, Du X, Chen Y, Xiong H, Ma C, Leng L, Young LH, Jorgensen WL, Li J, Bucala R. Limiting cardiac ischemic injury by pharmacological augmentation of macrophage migration inhibitory factor-AMP-activated protein kinase signal transduction. *Circulation* 2013;**128**:225–236.
27. Haemmerle G, Moustafa T, Woelkart G, Buttner S, Schmidt A, van de Weijer T, Hesselink M, Jaeger D, Kienesberger PC, Zierler K, Schreiber R, Eichmann T, Kolb D, Kotzbeck P, Schweiger M, Kumari M, Eder S, Schoiswohl G, Wongsiriroj N, Pollak NM, Radner FP, Preiss-Landl K, Kolbe T, Rulicke T, Pieske B, Trauner M, Lass A, Zimmermann R, Hoefler G, Cinti S, Kershaw EE, Schrauwen P, Madeo F, Mayer B, Zechner R. ATGL-mediated fat catabolism regulates cardiac mitochondrial function via PPAR-alpha and PGC-1. *Nat Med* 2011;**17**:1076–1085.
28. Holloway GP, Gurd BJ, Snook LA, Lally J, Bonen A. Compensatory increases in nuclear PGC1alpha protein are primarily associated with subsarcolemmal mitochondrial adaptations in ZDF rats. *Diabetes* 2010;**59**:819–828.
29. Miller EJ, Li J, Sinusas KM, Holman GD, Young LH. Infusion of a biotinylated bis-glucose photolabel: a new method to quantify cell surface GLUT4 in the intact mouse heart. *Am J Physiol Endocrinol Metab* 2007;**292**:E1922–E1928.
30. Sun W, Quan N, Wang L, Yang H, Chu D, Liu Q, Zhao X, Leng J, Li J. Cardiac-Specific Deletion of the Pdha1 Gene Sensitizes Heart to Toxicological Actions of Ischemic Stress. *Toxicol Sci* 2016;**151**:193–203.
31. Ma Y, Wang J, Gao J, Yang H, Wang Y, Manithody C, Li J, Rezaie AR. Antithrombin up-regulates AMP-activated protein kinase signalling during myocardial ischaemia/reperfusion injury. *Thromb Haemost* 2015;**113**:338–349.
32. Antman EM, Tanasijevic MJ, Thompson B, Schactman M, McCabe CH, Cannon CP, Fischer GA, Fung AY, Thompson C, Wybenga D, Braunwald E. Cardiac-specific troponin I levels to predict the risk of mortality in patients with acute coronary syndromes. *N Engl J Med* 1996;**335**:1342–1349.
33. Chen S, Zhu P, Guo HM, Solis RS, Wang Y, Ma Y, Wang J, Gao J, Chen JM, Ge Y, Zhuang J, Li J. Alpha1 catalytic subunit of AMPK modulates contractile function of cardiomyocytes through phosphorylation of troponin I. *Life Sci* 2014;**98**:75–82.
34. Ma Y, Li J. Metabolic shifts during aging and pathology. *Compr Physiol* 2015;**5**:667–686.
35. Russell RR III, Li J, Coven DL, Pypaert M, Zechner C, Palmeri M, Giordano FJ, Mu J, Birnbaum MJ, Young LH. AMP-activated protein kinase mediates ischemic glucose uptake and prevents postischemic cardiac dysfunction, apoptosis, and injury. *J Clin Invest* 2004;**114**:495–503.
36. Winnik S, Auwerx J, Sinclair DA, Matter CM. Protective effects of sirtuins in cardiovascular diseases: from bench to bedside. *Eur Heart J* 2015;**36**:3404–3412.
37. Jager S, Handschin C, St-Pierre J, Spiegelman BM. AMP-activated protein kinase (AMPK) action in skeletal muscle via direct phosphorylation of PGC-1alpha. *Proc Natl Acad Sci USA* 2007;**104**:12017–12022.
38. Amat R, Planavila A, Chen SL, Iglesias R, Giralt M, Villarroya F. SIRT1 controls the transcription of the peroxisome proliferator-activated receptor-gamma Co-activator-1alpha (PGC-1alpha) gene in skeletal muscle through the PGC-1alpha autoregulatory loop and interaction with MyoD. *J Biol Chem* 2009;**284**:21872–21880.
39. Pittelli M, Formentini L, Faraco G, Lapucci A, Rapizzi E, Cialdai F, Romano G, Moneti G, Moroni F, Chiarugi A. Inhibition of nicotinamide phosphoribosyltransferase: cellular bioenergetics reveals a mitochondrial insensitive NAD pool. *J Biol Chem* 2010; **285**:34106–34114.
40. Hasmann M, Schemainda I. FK866, a highly specific noncompetitive inhibitor of nicotinamide phosphoribosyltransferase, represents a novel mechanism for induction of tumor cell apoptosis. *Cancer Res* 2003;**63**:7436–7442.
41. Miller EJ, Li J, Leng L, McDonald C, Atsumi T, Bucala R, Young LH. Macrophage migration inhibitory factor stimulates AMP-activated protein kinase in the ischaemic heart. *Nature* 2008;**451**:578–582.

42. Muzumdar RH, Huffman DM, Calvert JW, Jha S, Weinberg Y, Cui L, Nemkal A, Atzmon G, Klein L, Gundewar S, Ji SY, Lavu M, Predmore BL, Lefer DJ. Acute humanin therapy attenuates myocardial ischemia and reperfusion injury in mice. *Arterioscler Thromb Vasc Biol* 2010;**30**:1940–1948.
43. Shibata R, Sato K, Pimentel DR, Takemura Y, Kihara S, Ohashi K, Funahashi T, Ouchi N, Walsh K. Adiponectin protects against myocardial ischemia-reperfusion injury through AMPK- and COX-2-dependent mechanisms. *Nat Med* 2005;**11**:1096–1103.
44. Solskov L, Magnusson NE, Kristiansen SB, Jessen N, Nielsen TT, Schmitz O, Botker HE, Lund S. Microarray expression analysis in delayed cardioprotection: the effect of exercise, AICAR, or metformin and the possible role of AMP-activated protein kinase (AMPK). *Mol Cell Biochem* 2012;**360**:353–362.
45. Hsu CP, Odewale I, Alcendor RR, Sadoshima J. Sirt1 protects the heart from aging and stress. *Biol Chem* 2008;**389**:221–231.
46. Hsu CP, Oka S, Shao D, Hariharan N, Sadoshima J. Nicotinamide phosphoribosyltransferase regulates cell survival through NAD+ synthesis in cardiac myocytes. *Circ Res* 2009;**105**:481–491.
47. Rane S, He M, Sayed D, Vashistha H, Malhotra A, Sadoshima J, Vatner DE, Vatner SF, Abdellatif M. Downregulation of miR-199a derepresses hypoxia-inducible factor-1alpha and Sirtuin 1 and recapitulates hypoxia preconditioning in cardiac myocytes. *Circ Res* 2009;**104**:879–886.
48. Shinmura K, Tamaki K, Bolli R. Impact of 6-mo caloric restriction on myocardial ischemic tolerance: possible involvement of nitric oxide-dependent increase in nuclear Sirt1. *Am J Physiol Heart Circ Physiol* 2008;**295**:H2348–H2355.
49. Mattagajasingh I, Kim CS, Naqvi A, Yamamori T, Hoffman TA, Jung SB, DeRicco J, Kasuno K, Irani K. SIRT1 promotes endothelium-dependent vascular relaxation by activating endothelial nitric oxide synthase. *Proc Natl Acad Sci USA* 2007;**104**:14855–14860.
50. Salminen A, Kaarniranta K. AMP-activated protein kinase (AMPK) controls the aging process via an integrated signaling network. *Ageing Res Rev* 2012;**11**:230–241.
51. Towler MC, Hardie DG. AMP-activated protein kinase in metabolic control and insulin signaling. *Circ Res* 2007;**100**:328–341.
52. Quan N, Sun W, Wang L, Chen X, Bogan JS, Zhou X, Cates C, Liu Q, Zheng Y, Li J. Sestrin2 prevents age-related intolerance to ischemia and reperfusion injury by modulating substrate metabolism. *FASEB J* 2017;**31**:4153–4167.
53. Alers S, Loffler AS, Wesselborg S, Stork B. Role of AMPK-mTOR-Ulk1/2 in the regulation of autophagy: cross talk, shortcuts, and feedbacks. *Mol Cell Biol* 2012;**32**:2–11.
54. He C, Klionsky DJ. Regulation mechanisms and signaling pathways of autophagy. *Annu Rev Genet* 2009;**43**:67–93.
55. El Messaoudi S, Rongen GA, de Boer RA, Riksen NP. The cardioprotective effects of metformin. *Curr Opin Lipidol* 2011;**22**:445–453.
56. Jiang Y, Huang W, Wang J, Xu Z, He J, Lin X, Zhou Z, Zhang J. Metformin plays a dual role in MIN6 pancreatic beta cell function through AMPK-dependent autophagy. *Int J Biol Sci* 2014;**10**:268–277.
57. Du Q, Jovanović S, Clelland A, Sukhodub A, Budas G, Phelan K, Murray-Tait V, Malone L, Jovanović A. Overexpression of SUR2A generates a cardiac phenotype resistant to ischemia. *FASEB J* 2006;**20**:1131–1141.
58. Gu C, Xing Y, Jiang L, Chen M, Xu M, Yin Y, Li C, Yang Z, Yu L, Ma H. Impaired cardiac SIRT1 activity by carbonyl stress contributes to aging-related ischemic intolerance. *PloS One* 2013;**8**:e74050.
59. Luo XY, Qu SL, Tang ZH, Zhang Y, Liu MH, Peng J, Tang H, Yu KL, Zhang C, Ren Z, Jiang ZS. SIRT1 in cardiovascular aging. *Clin Chim Acta* 2014;**437**:106–114.
60. Nakamura M, Bhatnagar A, Sadoshima J. Overview of pyridine nucleotides review series. *Circ Res* 2012;**111**:604–610.
61. Oka S, Hsu CP, Sadoshima J. Regulation of cell survival and death by pyridine nucleotides. *Circ Res* 2012;**111**:611–627.
62. Liu L, Wang P, Liu X, He D, Liang C, Yu Y. Exogenous NAD(+) supplementation protects H9c2 cardiac myoblasts against hypoxia/reoxygenation injury via Sirt1-p53 pathway. *Fundam Clin Pharmacol* 2014;**28**:180–189.
63. Vasto S, Candore G, Balistreri CR, Caruso M, Colonna-Romano G, Grimaldi MP, Listi F, Nuzzo D, Lio D, Caruso C. Inflammatory networks in ageing, age-related diseases and longevity. *Mech Ageing Dev* 2007;**128**:83–91.
64. Xie J, Zhang X, Zhang L. Negative regulation of inflammation by SIRT1. *Pharmacol Res* 2013;**67**:60–67.
65. Camici GG, Schiavoni M, Francia P, Bachschmid M, Martin-Padura I, Hersberger M, Tanner FC, Pelicci P, Volpe M, Anversa P, Lüscher TF, Cosentino F. Genetic deletion of p66(Shc) adaptor protein prevents hyperglycemia-induced endothelial dysfunction and oxidative stress. *Proc Natl Acad Sci USA* 2007;**104**:5217–5222.
66. Francia P, Delli Gatti C, Bachschmid M, Martin-Padura I, Savoia C, Migliaccio E, Pelicci PG, Schiavoni M, Lüscher TF, Volpe M, Cosentino F. Deletion of p66shc gene protects against age-related endothelial dysfunction. *Circulation* 2004;**110**:2889–2895.
67. Chen HZ, Wan YZ, Liu DP. Cross-talk between SIRT1 and p66Shc in vascular diseases. *Trends Cardiovasc Med* 2013;**23**:237–241.